의학박사 학위논문

Fat deposition in the tunica muscularis and decrease of interstitial cells of Cajal (ICC) and nNOS positive neuronal cells in the aged rat colon

노화에 따른쥐 대장 근층의 지방 축적과 카할 간질세포 및 nNOS 양성 신경세포의 감소

2014년 2월

서울대학교 대학원
의학과 내과학전공
조 현 진

2014년 조 현 진

의학박사 학위논문

노화에 따른 쥐 대장 근층의 지방 축적과 카할 간질세포 및 nNOS 양성 신경세포의 감소

2014 년 2 월

서울대학교 대학원

의학과 내과학전공

조 현 진

A thesis of the Degree of Doctor of Philosophy

Fat deposition in the tunica muscularis and decrease of interstitial cells of Cajal (ICC) and nNOS positive neuronal cells in the aged rat colon

February 2014

The Department of Internal Medicine,

Seoul National University

College of Medicine

Hyun Jin Jo

노화에 따른 쥐 대장 근층의 지방 축적과 카할 간질세포 및 nNOS 양성 신경세포의 감소

Fat deposition in the tunica muscularis and decrease of interstitial cells of Cajal (ICC) and nNOS positive neuronal cells in the aged rat colon

지도교수 김 주 성

이 논문을 의학박사 학위논문으로 제출함

2013 년 10 월

서울대학교 대학원
의학과 내과학 전공

조 현 진

조현진의 의학박사 학위논문을 인준함

2014 년 2 월

위 원 장 정 현 채 (인)

부위원장 김 주 성 (인)

위 원 김 나 영 (인)

위 원 김 상 균 (인)

위 원 김 유 선 (인)

Fat deposition in the tunica muscularis and decrease of interstitial cells of Cajal (ICC) and nNOS positive neuronal cells in the aged rat colon

by
Hyun Jin Jo

A thesis submitted to the Department of Internal Medicine in partial fulfillment of the requirements for the Degree of Doctor of Philosophy in Internal Medicine at Seoul National University College of Medicine

February 2014

Approved by Thesis Committee:

Professor Hyun Chae Jung Chairman
Professor Joo Sung Kim Vice chairman
Professor Maxoung Kim
Professor Kang Gyun Kim
Professor You Sun Kim

ABSTRACT

Fat deposition in the tunica muscularis and decrease of interstitial cells of Cajal (ICC) and nNOS positive neuronal cells in the aged rat colon

Introduction: Little is known about the time-course of aging on interstitial cells of Cajal (ICC) of colon. The aim of this study was to investigate the change of morphology, ICC and neuronal nitric oxide synthase (nNOS) immunoreactive cells in the aged rat.

Methods: The proximal colon of 344 Fischer rats at four different ages (6, 31, 74 weeks, and 2 years) were studied. The immunoreactivity of c-Kit, nNOS, anti-protein gene product 9.5(PGP 9.5) and synaptophysin were counted after immunohistochemistry. The *c-kit*, *SCF* (stem cell factor; ligand of Kit) and *nNOS* mRNA were measured by real-time PCR. c-Kit and nNOS protein were assessed by Western blot.

Isovolumetric contractile force measurement and electrical field stimulation (EFS) were conducted.

Results: The area of intramuscular fat deposition significantly increased with age after 31 weeks. c-Kit immunoreactive ICC and nNOS immunoreactive neurons and nerve fibers significantly declined with age. mRNA and protein expression of c-kit and nNOS decreased with aging. The functional study showed that the spontaneous contractility was decreased in aged rat, whereas EFS responses to atropine and L-NG-Nitroarginine methyl ester were increased in aged rat.

Conclusions: In conclusion, the decrease of proportion of proper smooth muscle, the density of ICC and nNOS immunoreactive neuronal fibers and the number of nNOS immunoreactive neurons during the aging process may explain the aging-associated colonic dysmotility.

Keywords: aging, colon, Interstitial cells of Cajal, nNOS, Rats, Inbred F344

Student number: 2011-30579

CONTENTS

LIST OF FIGURES

LIST OF ABBREVIATIONS

ICC: interstitial cells of Cajal

nNOS: neuronal nitric oxide synthase

SCF: stem cell factor

EFS: electrical field stimulation

NO: nitric oxide

IHC: immunohistochemistry

H&E: hematoxylin and eosin

sGAG : sulfated glycosaminoglycan

LPO: lipid hydroperoxide

SMB: submucosal border

CM: circular muscle

MP: myenteric plexus

LM: longitudinal muscle

KRB: Krebs-Ringer bicarbonate

AUC: area under the curve

NANC: non-adrenergic non-cholinergic

Introduction

Aging leads to the impairment of organ function as a result of accumulation of diverse deleterious changes throughout the cells and tissues (1). Constipation is a common problem in the elderly and known to be associated with multiple factors, such as decreased intestinal secretory epithelial function, abnormal colonic motility caused by enteric neurodegeneration and reduced contractile response of smooth muscle cells with age (2-4).

Enteric neurodegeneration involves the loss of enteric neuron, especially, excitatory cholinergic neurons (5). In contrast, nitrergic myenteric neurons are known to be selectively spared in the aged (6-8). However, there was a contrary report that nitrergic neurons decreased in the aged rats (9). Nitrergic enteric neurons, which release nitric oxide (NO) generated by catalysis of neuronal nitric oxide synthase (nNOS), act as non-adrenergic, non-cholinergic inhibitory neuron and induce colonic smooth muscle relaxation (10). This NO is known to enhance transit of the rat colon by mediating descending relaxation, which in turn facilitates propulsion of the colonic

contents(11). Nitrergic nerves of colon may be an important component of colonic motility.

Interstitial cells of Cajal (ICC) also play important roles in gastrointestinal motility. ICC play as an electrical pacemaker as well as mediate both inhibitory and excitatory motor neurotransmissions which manifest as electrical slow waves in smooth muscles. Consequently, ICC contribute to segmenting and peristaltic contractile activity (12, 13). ICC have been diminished or lost in human disease for such as diabetic gastroenteropathy (14), slow transit constipation (15-17) and intestinal pseudo-obstruction (18). It is well known that ICC express proto-oncogene *c-kit* (19, 20). The stem cell factor (SCF) is natural ligand of Kit (21) and involves the development and maintenance of ICC (22). It has been known that the expression of *c-kit* mRNA and c-Kit protein significantly decreased in the colon of slow transit constipation patient and diabetes mellitus mouse (21, 23). In addition, there was a study on the number and volume of ICC networks in the normal human stomach and colon which declined with aging (24). In one study using progeric mouse, the percentage of ICC did not change and network volume of ICC decreased in the

proximal colon (25). However, a few data have been reported on the time-course of age related changes about ICC in the colon of conventional rats, so far. Furthermore, the results about age-related changes of nitrergic neurons are inconsistent. Previously, we reported that the lower part of rat gastric mucosa was replaced by connective tissue with accumulation of oxidative products with age (26). Similarly, we presumed a hypothesis that a certain morphologic change might occur in the colonic tissue with aging.

From this background, we aimed to assess the morphologic change and the changes of number and molecular expression of ICC, nNOS immunoreactive neurons and neuronal fibers in the proximal colon of rat at four different ages using immunohistochemistry (IHC) and molecular analysis.

Materials and Methods

Animals and tissue preparation.

Specific pathogen free, 344, male, Fischer rats (6-, 31-, 74-weeks and 2 years of age) were used (Orient Co. Ltd., Seoul, Korea). The animals were housed in a cage maintained at 23℃, with 12:12-hour light-dark cycles under specific pathogen-free conditions. The rats were starved but allowed for water for 12 hours prior to the experiments. The animals were anesthetized by zoletil and rompun mixture and killed by decapitation. One cm length of the proximal colon per each rat was obtained and fixed in 10% buffered formalin for histology. The specimens were embedded in paraffin and sectioned perpendicularly to the lumen (section thickness, 4 μm) and stained with hematoxylin and eosin (H&E). This study was approved by the Institutional Animal Care and Use Committee (IACUC) of Seoul National University Bundang Hospital.

Muscular histology.

The histology was evaluated by pathologist (H.S.L) blinded to

the age of the animal. The one H&E stained slide per rat (each age group, n = 5) and the two fields per slide were randomly selected. The area of the total smooth muscle, fatty tissue and proper muscle in the tunica muscularis of colon was quantified using the Image- Pro® Plus analysis system (Media Cybernetics, Inc., San Diego, CA, USA). The area was expressed as mm^2 per field of view.

Immunohistochemistry for c-Kit, nNOS, PGP(protein gene product)9.5 and synaptophysin.

For the c-Kit, nNOS, PGP 9.5 and synaptophysin IHC, the sections were incubated with the following primary antibody: anti-c-Kit antibody (dilution 1:100; polyclonal rabbit anti-human CD117, DAKO, Glostrup, Denmark), anti-nNOS antibody (dilution 1:500; AB5380 Chemicon, Millipore Corporation, Billerica, MA, USA), anti-PGP 9.5 antibody (dilution 1:250; CM 329 AK, Biocare Mecial, CA, USA) and anti-synaptophysin antibody (dilution 1:150; monoclonal mouse anti-human synaptophysin, clone SY38, DAKO, Glostrup, Denmark) after deactivation of endogenous peroxidase with 3% hydrogen peroxide and blocking of nonspecific binding sites. The

immunostain was performed using an automatic immunostainer (BenchMark XT, Ventana Medical Systems, Inc., Tucson, AZ, USA) according to the manufacturer's instructions. UltraView Universial DAB detection kit (Ventana Medical Systems) was used as secondary antibody. The negative control for IHC was performed without primary antibody.

The immunostained tissues were examined under a light microscope (Carl Zeiss, Jena, Germany) linked to a computer-assisted image analysis system (AxioVision Rel.4.8; Carl Zeiss). Two immunostained slides (one slide for synaptophysin) per each rat (each age group, n = 6) was made and four to five fields per slide were randomly selected and micrographed at x200. The micrograph was divided into four anatomic regions; submucosal border (SMB), circular muscle (CM), myenteric plexus (MP) and longitudinal muscle (LM) region (27) using Adobe photoshop ver. 7.0 (Adobe systems; Mountain View, CA, USA). Finally, quantitative assessment of c-Kit, nNOS, PGP 9.5 and synaptophysin immunoreactivity was performed using the Image- Pro® Plus analysis system and measurements were expressed as proportion of immunoreactive area (% of total area). Mast cells, which are known to express c-Kit but could

be identified by their round or oval shape and lack of processes, were excluded from the counts (14, 20, 24). Ganglia in the myenteric plexus were micrographed at x1000. The number of myenteric neurons, which include nucleus was enumerated.

Real-time PCR for c-kit, SCF and nNOS.

c-kit, *SCF* and *nNOS* mRNA were measured by real-time PCR (28). Briefly, RNA was extracted from the proximal colonic muscle tissues devoid of the mucosa, submucosa and preferably serosa using the RNeasy Plus Mini kit (Qiagen, Valencia, CA, USA) according to the manufacturer's instructions. RNA samples were diluted to a final concentration of 0.5 mg mL^{-1} in RNase-free water and stored at −80℃ until use. Synthesis of the cDNA was performed with 1 mg of total RNA with M-MLV reverse transcription reagents (Invitrogen, Carlsbad, CA, USA). The 20 μl reverse transcription reaction was consisted of 4 μl of first-strand buffer, 500 mM deoxynucleoside triphosphate mixture, 2.5 mM oligo(dT) 12-18 primer, 0.4 U mL^{-1}ribonuclease inhibitor, and 1.25 U mL^{-1}Moloney murine leukemia virus reverse transcriptase (Invitrogen). The thermal cycling parameters for the reverse transcription were 10

minutes at 65℃, 50 minutes at 37℃ and 15 minutes at 70℃. Real-time PCR amplification and determination were performed using SYBR Premix Ex TaqTM (Takara Bio, Shiga, Japan) according to manufacturer's protocols.

The following primers were used: *c-kit* forward, TTC CTG TGA CAG CTC AAA CG; *c-kit* reverse, AGC AAA TCT TCC AGG TCC AG; *SCF* forward, CAA AAC TGG TGG CGA ATC TT; *SCF* reverse, GCC ACG AGG TCA TCC ACT AT; *nNOS* forward, CTA CAA GGT CCG ATT CAA CAG; *nNOS* reverse, CCC ACA CAG AAG ACA TCA CAG; *GAPDH* forward, AGG TGA AGG TCG GAG TCA; and *GAPDH* reverse, GGT CAT TGA TGG CAA CAA. The *GAPDH* gene was used as an endogenous reference as a control for expression independent sample-to-sample variability. The amplification protocol consists of an initial denaturation step at 95℃ for 10 seconds followed by 40 cycles of denaturation for 5 seconds at 95℃ and annealing/extension of 33 seconds at 55℃. Relative expressions of target genes were normalized by dividing the target Ct values by the endogenous Ct values. All equipments were purchased from Applied Biosystems and used according to their protocols. RNA-free water was used in Real-time PCR as

no-template controls (NTC). After amplification, we performed melting curve analysis using ABI PRISM® 7000 Sequence Detection System software (Applied Biosystems).

Western blotting for c-Kit and nNOS.

The proximal colonic muscle tissue devoid of mucosa, submucosa and preferably serosa was homogenized with lysis buffer containing 25 mMTris-HCL (pH 7.4), EGTA (1 mM), DTT (1 mM), leupeptin (10 μg mL^{-1}), aprotinin (10 μg mL^{-1}), PMSF (1 mM), and Triton X-100 (0.1%). Briefly, the proteins (each sample, 100 μg) were separated by SDS-PAGE (8% wt/wt gel) and transferred to PVDF membranes. All procedures were performed in Tris buffer (40 mM, pH 7.55) containing 0.3 M of NaCl and 0.3% Tween 20. The membranes were then blocked with dried milk (5% wt/vol) and subsequently incubated with c-Kit (1:100; rabbit polyclonal antibody, Santa Cruz Biotechnology, Santa Cruz, CA, USA), nNOS (1:500; mouse monoclonal IgG2a antibody, BD Biosciences, San Diego, CA, USA) and β-actin (1:1000; rabbit polyclonal antibody, Biovision, Milpitas, CA, USA) at 4°C overnight. The blots were incubated with secondary antibody (rabbit polyclonal antibody, Santa Cruz

Biotechnology for c-Kit (dilution 1:500) and β-actin(dilution 1:1000), mouse polyclonal antibody, 1:1000; Santa Cruz Biotechnology for nNOS) and an imaging analyzer was used to measure the band densities. For c-Kit immunoblot, each of the optical density of mature (145 kDa) and immature (120 kDa) forms was combined into one in the analysis process using densirometry(29).

Isometric force measurements and electrical field stimulation.

Mechanical responses were performed to investigate the functional difference of colon between 6- weeks and 2-years-old F344 rats using standard organ-bath techniques. Segments of the proximal colon were removed through a midline abdominal incision and opened along the mesenteric border. Luminal contents were removed by washing with Krebs–Ringer bicarbonate solution (KRB), and the mucosa was removed leaving the tunica muscularis and remnants of the submucosa. The muscles were mounted under 1 g tension and then allowed to equilibrate for 1–2 hours with constant perfusion with fresh KRB. The spontaneous contractile activity was measured by

area under the curve (AUC) at the resting state and then electrical field stimulation (EFS, 5 Hz, 320 mA, 1 ms for 30 seconds) was performed to induce neural response with parallel platinum wire electrodes to colonic muscle strips. The contraction and relaxation responses by EFS of colonic muscle were measured under atropine (10 μM) sequentially. And the EFS responses to apamin (1 μM) and L-NG-Nitroarginine methyl ester (L-NAME, 10 μM) were determined under non-adrenergic non-cholinergic (NANC) condition by adding atropine, propranolol, and phentolamine (each 1 μM). All data were recorded using the PowerLab data acquisition system. Using the recorded waveform, the AUC was calculated by integrating the differences between the maximum and minimum values obtained immediately before and after the EFS stimulation. When measuring the percent changes of EFS response under drug pretreatment, the value before the drug treatment was defined as 100%.

Statistical analysis.

All statistical calculations were performed using SPSS software (version 18.0; SPSS Inc., Chicago, IL, USA). The

results were compared by the Mann-Whitney U-test and the Wilcoxon's rank-sum test. All values are reported as means ± SE. A $P < 0.05$ was considered statistically significant.

Results

Influence of aging on intramuscular fat deposition.

The total area of tunica muscularis of the proximal colon significantly increased with age (Fig. 1). However, most of this increase was originated from the deposition of intramuscular fat with age ($P < 0.001$) (Fig. 1). There was no fat deposition in 6-week, but observed only in one field in 31-weeks-old. However, fat deposition was observed in all fields of 74-weeks-old and 2-years-old rat. There was no significant change in proper smooth muscle area ($P = 0.296$).

Influence of aging on ICC.

The proportion of c-Kit-positive area decreased with aging. That of 2-years-old rat was significantly decreased compared to 6-, 31- and 74-weeks-old rat in SMB, CM and MP (SMB, $P < 0.001$ vs. 6 and 31 weeks, $P = 0.013$ vs. 74 weeks; CM, $P < 0.001$ vs. 6 and 31 weeks, $P = 0.002$ vs. 74 weeks; MP, $P < 0.001$ vs. 6 weeks, $P = 0.001$ vs. 31 weeks, $P = 0.003$ vs. 74 weeks). Also, the proportion of c-Kit-positive area of 31-

weeks and 74-weeks-old rat was significantly lower than that of 6-weeks-old rats in all area (31 weeks, P = 0.046, P = 0.019, P = 0.007 and P = 0.007; 74 weeks, all P < 0.001 in SMB, CM, MP and LM) (Fig. 2).

c-kit mRNA expression decreased with aging. That of 2-years-old rats significantly decreased compared to the 6-weeks-old rats (P = 0.035) (Fig. 3*A*). Similarly, *SCF* mRNA expression of 74-weeks and 2-years-old rats was significantly lower than that of 6-weeks-old rats (P = 0.048, P = 0.002, respectively) (Fig. 3*B*). c-Kit protein expression was the highest in 6-weeks-old rats and decreased with aging. c-Kit protein expression of 74-weeks and 2-years old rats was significantly lower than that of 6-weeks-old rats (P = 0.015 and P = 0.029, respectively) (Fig. 3*C*).

Influence of aging on nNOS positive neurons and immunoreactivity of PGP 9.5 and synaptophysin .

Similar to c-Kit immunostain, a larger proportion of nNOS-positive area was present in the 6 weeks old and it rapidly decreased with age (Fig. 4*A*) In SMB, CM and MP, the proportion of nNOS-positive area of 2-years-old rats was

significantly lower than that of 6-, 31- and 74-weeks-old rats (SMB and CM, all $P < 0.001$; MP, $P = 0.002$, $P = 0.004$ and $P = 0.027$).That of 74-weeks-old rats was significantly lower compared to 6- and 31-weeks-old rats in SMB ($P < 0.001$and $P = 0.015$, respectively). For CM and LM, nNOS-positive area of 31- and 74 weeks-old rats was lower than that of 6-weeks-old rats with statistical significance (CM, both $P < 0.001$; LM, $P = 0.002$ and $P = 0.013$) (Fig. 4*B*). In terms of *nNOS* mRNA expression, 2-years-old rats showed significant decrease compared to the 6-weeks-old rats ($P = 0.015$) (Fig. 5*A*). nNOS protein expression was lower in 74-weeks and 2-years-old rats than that of the 6- and 31-weeks-old rats and there was statistical significance (In 74 weeks, all $P < 0.001$; In 2 years, $P = 0.003$ vs. 6 weeks, $P = 0.013$ vs. 31 weeks) (Fig. 5*B*).

When myenteric ganglion was analyzed (Fig. 6*A*), the percent of nNOS-positive neuronal cell per total neuronal cell was also decreased as age increased (Fig. 6*B*). The proportion of nNOS-immunoreactive area of 74-weeks and 2-years-old rats were also significantly lower than 6- and 31-weeks-old rats (Fig. 6*C*).

PGP 9.5 immuno-positive area of 31-weeks-old rats was most high compared to other age groups in SMB, CM, MP and LM. PGP 9.5 immuoreactivity of 74-weeks and 2-years old rats was similar or slightly higher than 6-weeks-old rats (Fig 7*A* and 7*B*). However, for the relative ratio of nNOS-positive area to PGP 9.5-positive area, 6-weeks-old rats showed the peak level with statistical significance and the relative ratio of nNOS/PGP 9.5 of 2-years-old rats was lower than that of other age groups (In SMB and CM, both $P < 0.001$ vs. 6 weeks, $P = 0.017$ and $P = 0.001$ vs. 31 weeks, $P = 0.004$ and $P < 0.001$ vs. 74 weeks; in MP, $P < 0.001$ vs. 6 weeks) (Fig 7*C*).

The proportion of synaptophysin-positive area generally tended to decrease with age except LM (Fig. 8*A* and 8*B*) and the ratio of nNOS-positive area to synaptophysin-positive area was also significantly lower in the aged rats compared to young rats (Fig. 8*C*). The proportion of synaptophysin-positive area of 2-years-old rats was significantly lower than that of 6-weeks-old rats in SMB ($P = 0.016$) and 74-weeks-old rats in MP ($P = 0.015$). In CM, the proportion of synaptophysin-positive area of 2-years-old rat was significantly decreased compared with other groups ($P < 0.001$ compared to 6 weeks

and 31 weeks, and P = 0.005 compared to 74 weeks). In addition, the ratio of nNOS to synaptophysin of 74−weeks and 2−years−old rats was decreased compared to 6−weeks−old rats in CM (P = 0.044 in 74weeks, P = 0.008 in 2 years) and MP (P = 0.003 in 74 weeks, P = 0.011 in 2 years). In SMB, the ratio of nNOS to synaptophysin of 2−years−old rats was lower than that of 6−weeks and 31−weeks−old rats (P = 0.004 to 6 weeks, P < 0.001 to 31 weeks). As there were cases that the value of nNOS, PGP 9.5 or synatophysin−positive area was zero in LM, the statistical analysis was not performed in LM.

Influence of aging on colonic motility.

The AUC of colonic spontaneous contraction in 2−years−old rats, measured by isometric force measurement, was significantly decreased compared with the 6−weeks−old rats (6−weeks−old, 325.8 ± 8.9 mN x min vs. 2−years−old, 287.2 ± 17.3 mN x min) (P = 0.032) (Fig. 9*A*). The contractile response to EFS of 2−years−old rats was significantly inhibited by atropine compared with the 6−weeks−old rats (6−weeks−old, 92.5±5.9 % vs. 2−years−old, 19.2 ± 9.7) (P = 0.000) (Fig. 9*B*). Under the NANC condition, apamin

pretreatment did not affect the response to EFS in both aged rat colon (6-weeks-old, 116.9±40.2 % vs. 2-years-old, 97.0 ±24.4), however L-NAME pretreatment significantly increased contractility in 2-years-old rats compared with the 6-weeks-old rats (6-weeks-old, 129.8±35.0 % vs. 2-years-old, 205.1±33.7) (P = 0.000) (Fig. 9*C*).

Discussion

When we assessed the morphologic and molecular changes of ICC and nNOS-positive enteric neurons in the rat colon using four different age groups of 344 Fischer rats, the most peculiar finding was thickening of muscular layer with age, which was originated from fat deposit. These changes have not been reported in human as well as experimental animals, so far. The mechanism of fat deposition in colonic smooth muscle of rat including oxidative stress and its effects on the contraction are needed to be investigated in the future.

Several studies demonstrated that the number of myenteric neurons of the rat colon decreased with aging (30). However, the loss of enteric neurons was mainly cholinergic neurons, and nNOS-positive nitrergic neurons were known to be relatively spared (5, 6, 30-32). In the preset study, the relative ratio of nNOS/PGP 9.5 immunoreactivity and the percent of nNOS-positive neuronal cell per total neuronal cell were analyzed to exclude the dilution effect by growth. The result clearly showed the decrease of nNOS-immunoreactive neuronal cells

with age, which might be related to the damage of nitrergic neurons, such as axonal swelling and loss of expression of NOS in aged rats (7, 9). Similarly, aging gastric mucosa has shown reduced nNOS activity (26, 33). The decrease of nNOS-positivity was found to be originated from the selective loss of nNOS neurons. Even though this result could not completely exclude the possibility of loss of nNOS enzyme expression with aging, the decrease of relative ratio of nNOS/PGP 9.5-immunoreactivity together with the decline of the percent of nNOS-positive neuronal cell per total neuronal cell might suggest the loss of nitrergic neurons in the old aged rats.

The ICC are necessary for maintaining gastrointestinal motility. The decrease of ICC, as observed in several motility disorders (14-16, 18, 34, 35), reduces amplitudes of slow wave, consequently, induces intestinal dysmotility by reducing electrical drive to smooth muscle contractions and peristalsis (36). Recent study has shown that the number and volume of ICC networks in the normal human stomach and colon declined with age using IHC analysis but related molecular analysis, such as Western immunoblotting or real-time PCR, was absent in that study (24). Similarly, the ICC network volumes were

reduced in proximal colon of progeric mice, but little is known about the time course of age-related changes on ICC in conventional rat model (23, 28). In the present study the proportion of c-Kit-positive area, the largest of which located at the region of the MP, clearly decreased with aging. This depletion of c-Kit-positive ICC was diffuse across the layers of the rat colon. As ICC is an important factor of gastrointestinal motility, the diffuse reduction of density of ICC with age may explain the aging-associated colonic dysmotility.

The SCF/*c-kit* signal pathway is critical in the normal development, maturation, and phenotype maintenance of ICC (37-40). The primary loss of intramuscular ICC and reduction in myenteric ICC were noted not only in *kit* mutant mice (W/W^V) (41) but also in SCF mutant Sl/Sl^d mice (42). However, the underlying mechanism for the decrease of ICC with age is not well known yet. Recent study on the stomach of progeric mice suggested that the loss of ICC with age was dependent on multiple factors such as reduction in SCF, low circulating insulin and IGF-I levels and increased oxidative stress (31). In the present study, the expression of *c-kit* mRNA and c-Kit protein was decreased with aging. Another molecular work in the

present study, *SCF* mRNA also showed a good correlation of decreasing pattern with the c-Kit protein and *c-kit* mRNA expression. These results together with the previous reports (21, 40, 43) suggest that the SCF preferentially contributes to expression of c-Kit-positive ICC.

In addition to activation of the c-kit receptor via SCF, the release of neuronal nitric oxide is also known to increase proliferation of ICC in mice (44, 45). In the study using stomach body tissue of mouse, ICC volume and c-Kit protein of neuronal $NOS^{-/-}$ mouse were decreased than control. Additionally, number of ICC in primary cell culture and organotypic culture were increased by nitric oxide donor (46). Furthermore, there was a report that nitrergic enteric neurons act as a source of SCF (47). In the present study, nNOS-positive neurons and neuronal fibers of the rat proximal colon as well as the expression of nNOS protein decreased with age. Similarly, the *nNOS* mRNA of 2-years-old rats was significantly lower than that of 6-weeks-old rats. Since the nNOS-derived NO is important for the presence of ICC in the gastrointestinal tract (48), the loss of nNOS-positive neuronal

cells in the aged rat colon might cause adverse effect on ICC maintenance.

There are also other evidences that oxidative stress may induce loss of ICC or nNOS. For example, Klotho-deficient progeric mice showed profound ICC loss, but Klotho protected ICC by limiting oxidative stress (31). In addition, c-Kit and nNOS expressions were lost during diabetic gastroparesis due to increased levels of oxidative stress caused by low levels of heme oxygenase-1, an important cytoprotective molecule against oxidative injury (49). We detected that colonic mucosal LPO, although it was measured in the mucosa (data was not shown), increased during the aging process. Taken together the decrease of density of ICC and nNOS in the rat colon with aging also could be a consequence of oxidative stress.

EFS for evaluation of functional difference between 6-weeks and 2-years old rats showed that spontaneous colonic muscle contraction at resting state significantly decreased in the aged rat , although the difference between two age groups was very small (Fig. 9*A*). The decreased spontaneous activities in 2-years-old rats might be affected by both the damage of ICC and the degeneration of enteric neuron with aging. The

response to EFS under the treatment of atropine (Fig. 9*B*) or L-NAME (Fig. 9*C*) was different between two age groups. Both the relative decline of contractile response to EFS under the atropine pretreatment and the relative increment of contractile response to EFS under the L-NAME were significantly larger in aged rats compared with young rats (Fig. 9*B* and 9*C*). It is well known that atropine and L-NAME inhibit the action of excitatory cholinergic and inhibitory nitrergic neuron, respectively (50, 51). Therefore, it would be possible that the relatively increased response to atropine and L-NAME in the aged rats could reflect the degeneration of cholinergic and nitrergic neuron, respectively. However, this explanation needs further experiment.

We used the image analyzer to quantify ICC and nNOS-positive neuronal structures. This method offered several advantages over conventional cell counting techniques. That is, it allowed cell density to be determined in areas with difficulty in identifying individual cells due to high density. The strong point of this study is that we showed the age-related changes of density and molecular expression of ICC and nNOS-positive enteric neurons in the rat colon in four different ages using IHC

study together with molecular analysis. In conclusion, the proportion of proper smooth muscle in the tunica muscularis, the density of ICC and nNOS-immunoreactive neuronal fibers and the number of nNOS-immunoreactive neurons were decreased during the aging process in the proximal colon of rat. This change might cause impairment of colonic smooth muscle contraction and could be one mechanism for constipation in the elderly. Additional functional and physiologic study, which might provide a direct relationship, is currently underway.

References

1. **Harman D.** Aging: overview. *Ann N Y Acad Sci* 928: 1-21, 2001.
2. **Bitar KN, and Patil SB.** Aging and gastrointestinal smooth muscle. *Mech Ageing Dev* 125: 907-910, 2004.
3. **Braaten B, Madara JL, and Donowitz M.** Age-related loss of nongoblet crypt cells parallels decreased secretion in rabbit descending colon. *Am J Physiol* 255: G72-84, 1988.
4. **Camilleri M, Cowen T, and Koch TR.** Enteric neurodegeneration in ageing. *Neurogastroenterol Motil* 20: 418-429, 2008.
5. **Bernard CE, Gibbons SJ, Gomez-Pinilla PJ, Lurken MS, Schmalz PF, Roeder JL, Linden D, Cima RR, Dozois EJ, Larson DW, Camilleri M, Zinsmeister AR, Pozo MJ, Hicks GA, and Farrugia G.** Effect of age on the enteric nervous system of the human colon. *Neurogastroenterol Motil* 21: 746-e746, 2009.
6. **Cowen T, Johnson RJ, Soubeyre V, and Santer RM.** Restricted diet rescues rat enteric motor neurones from age related cell death. *Gut* 47: 653-660, 2000.
7. **Phillips RJ, Kieffer EJ, and Powley TL.** Aging of the myenteric plexus: neuronal loss is specific to cholinergic neurons. *Auton Neurosci* 106: 69-83, 2003.
8. **Wade PR, and Cowen T.** Neurodegeneration: a key factor in the ageing gut. *Neurogastroenterol Motil* 16 Suppl 1: 19-23, 2004.
9. **Takahashi T, Qoubaitary A, Owyang C, and Wiley JW.** Decreased expression of nitric oxide synthase in the colonic myenteric plexus of aged rats. *Brain Res* 883: 15-21, 2000.

10. **Takahashi T, and Owyang C.** Regional differences in the nitrergic innervation between the proximal and the distal colon in rats. *Gastroenterology* 115: 1504-1512, 1998.
11. **Mizuta Y, Takahashi T, and Owyang C.** Nitrergic regulation of colonic transit in rats. *Am J Physiol* 277: G275-279, 1999.
12. **Huizinga JD.** Gastrointestinal peristalsis: joint action of enteric nerves, smooth muscle, and interstitial cells of Cajal. *Microsc Res Tech* 47: 239-247, 1999.
13. **Nakagawa T, Misawa H, Nakajima Y, and Takaki M.** Absence of peristalsis in the ileum of W/W(V) mutant mice that are selectively deficient in myenteric interstitial cells of Cajal. *J Smooth Muscle Res* 41: 141-151, 2005.
14. **Nakahara M, Isozaki K, Hirota S, Vanderwinden JM, Takakura R, Kinoshita K, Miyagawa J, Chen H, Miyazaki Y, Kiyohara T, Shinomura Y, and Matsuzawa Y.** Deficiency of KIT-positive cells in the colon of patients with diabetes mellitus. J Gastroenterol Hepatol 17: 666-670, 2002.
15. **Geramizadeh B, Hayati K, Rahsaz M, and Hosseini SV.** Assessing the interstitial cells of Cajal, cells of enteric nervous system and neurotransmitters in slow transit constipation, using immunohistochemistry for CD117, PGP9.5 and serotonin. *Hepatogastroenterology* 56: 1670-1674, 2009.
16. **He CL, Burgart L, Wang L, Pemberton J, Young-Fadok T, Szurszewski J, and Farrugia G.** Decreased interstitial cell of cajal volume in patients with slow-transit constipation. *Gastroenterology* 118: 14-21, 2000.
17. **Lee JI, Park H, Kamm MA, and Talbot IC.** Decreased density of interstitial cells of Cajal and neuronal cells in patients

with slow-transit constipation and acquired megacolon. *J Gastroenterol Hepatol* 20: 1292-1298, 2005.

18. **Isozaki K, Hirota S, Miyagawa J, Taniguchi M, Shinomura Y, and Matsuzawa Y.** Deficiency of c-kit+ cells in patients with a myopathic form of chronic idiopathic intestinal pseudo-obstruction. *Am J Gastroenterol* 92: 332-334, 1997.
19. **Chen H, Redelman D, Ro S, Ward SM, Ordog T, and Sanders KM.** Selective labeling and isolation of functional classes of interstitial cells of Cajal of human and murine small intestine. *Am J Physiol Cell Physiol* 292: C497-507, 2007.
20. **Ward SM, and Sanders KM.** Physiology and pathophysiology of the interstitial cell of Cajal: from bench to bedside. I. Functional development and plasticity of interstitial cells of Cajal networks. *Am J Physiol Gastrointest Liver Physiol* 281: G602-611, 2001.
21. **Yamamoto T, Watabe K, Nakahara M, Ogiyama H, Kiyohara T, Tsutsui S, Tamura S, Shinomura Y, and Hayashi N.** Disturbed gastrointestinal motility and decreased interstitial cells of Cajal in diabetic db/db mice. *J Gastroenterol Hepatol* 23: 660-667, 2008.
22. **Ordog T, Hayashi Y, and Gibbons SJ.** Cellular pathogenesis of diabetic gastroenteropathy. *Minerva Gastroenterol Dietol* 55: 315-343, 2009.
23. **Tong WD, Liu BH, Zhang LY, Xiong RP, Liu P, and Zhang SB.** Expression of c-kit messenger ribonucleic acid and c-kit protein in sigmoid colon of patients with slow transit constipation. *Int J Colorectal Dis* 20: 363-367, 2005.
24. **Gomez-Pinilla PJ, Gibbons SJ, Sarr MG, Kendrick ML, Shen KR, Cima RR, Dozois EJ, Larson DW, Ordog T, Pozo MJ, and Farrugia G.** Changes in interstitial cells of cajal with age in the human stomach and colon. *Neurogastroenterol Motil* 23: 36-44, 2011.

25. Asuzu DT, Hayashi Y, Izbeki F, Popko LN, Young DL, Bardsley MR, Lorincz A, Kuro OM, Linden DR, Farrugia G, and Ordog T. Generalized neuromuscular hypoplasia, reduced smooth muscle myosin and altered gut motility in the klotho model of premature aging. *Neurogastroenterol Motil* 23: e309-323, 2011.
26. Kang JM, Kim N, Kim JH, Oh E, Lee BY, Lee BH, Shin CM, Park JH, Lee MK, Nam RH, Lee HE, Lee HS, Kim JS, Jung HC, and Song IS. Effect of aging on gastric mucosal defense mechanisms: ROS, apoptosis, angiogenesis, and sensory neurons. *Am J Physiol Gastrointest Liver Physiol* 299: G1147-1153, 2010.
27. Wang XY, Huizinga JD, Diamond J, and Liu LWC. Loss of intramuscular and submuscular interstitial cells of Cajal and associated enteric nerves is related to decreased gastric emptying in streptozotocin-induced diabetes. *Neurogastroenterol Motil* 21: 2009.
28. Mansuroglu T, Ramadori P, Dudas J, Malik I, Hammerich K, Fuzesi L, and Ramadori G. Expression of stem cell factor and its receptor c-Kit during the development of intrahepatic cholangiocarcinoma. *Lab Invest* 89: 562-574, 2009.
29. D'Allard D, Gay J, Descarpentries C, Frisan E, Adam K, Verdier F, Floquet C, Dubreuil P, Lacombe C, Fontenay M, Mayeux P, and Kosmider O. Tyrosine kinase inhibitors induce down-regulation of c-Kit by targeting the ATP pocket. *PloS one* 8: e60961, 2013.
30. Santer RM, and Baker DM. Enteric neuron numbers and sizes in Auerbach's plexus in the small and large intestine of adult and aged rats. *J Auton Nerv Syst* 25: 59-67, 1988.
31. Izbeki F, Asuzu DT, Lorincz A, Bardsley MR, Popko LN, Choi KM, Young DL, Hayashi Y, Linden DR, Kuro-o M, Farrugia G,

and Ordog T. Loss of Kitlow progenitors, reduced stem cell factor and high oxidative stress underlie gastric dysfunction in progeric mice. *J Physiol* 588: 3101-3117, 2010.

32. Sekiya M, Hiraishi A, Touyama M, and Sakamoto K. Oxidative stress induced lipid accumulation via SREBP1c activation in HepG2 cells. *Biochem Biophys Res Commun* 375: 602-607, 2008.
33. Miyake H, Inaba N, Kato S, and Takeuchi K. Increased susceptibility of rat gastric mucosa to ulcerogenic stimulation with aging. Role of capsaicin-sensitive sensory neurons. *Dig Dis Sci* 41: 339-345, 1996.
34. Kim SJ, Park JH, Song DK, Park KS, Lee JE, Kim ES, Cho KB, Jang BK, Chung WJ, Hwang JS, Kwon JG, and Kim TW. Alterations of colonic contractility in long-term diabetic rat model. *J Neurogastroenterol Motil* 17: in press, 2011.
35. Lee HT, Hennig GW, Park KJ, Bayguinov PO, Ward SM, Sanders KM, and Smith TK. Heterogeneities in ICC Ca2+ activity within canine large intestine. *Gastroenterology* 136: 2226-2236, 2009.
36. Sanders KM, Koh SD, and Ward SM. Interstitial cells of cajal as pacemakers in the gastrointestinal tract. *Annu Rev Physiol* 68: 307-343, 2006.
37. Hirota S, Isozaki K, Nishida T, and Kitamura Y. Effects of loss-of-function and gain-of-function mutations of c-kit on the gastrointestinal tract. *J Gastroenterol* 35 Suppl 12: 75-79, 2000.
38. Lin L, Xu LM, Zhang W, Ge YB, Tang YR, Zhang HJ, Li XL, and Chen JD. Roles of stem cell factor on the depletion of interstitial cells of Cajal in the colon of diabetic mice. *Am J Physiol Gastrointest Liver Physiol* 298: G241-247, 2010.
39. Rich A, Miller SM, Gibbons SJ, Malysz J, Szurszewski JH, and Farrugia G. Local presentation of Steel factor increases

expression of c-kit immunoreactive interstitial cells of Cajal in culture. *Am J Physiol Gastrointest Liver Physiol* 284: G313-320, 2003.

40. **Wu JJ, Rothman TP, and Gershon MD**. Development of the interstitial cell of Cajal: origin, kit dependence and neuronal and nonneuronal sources of kit ligand. *J Neurosci Res* 59: 384-401, 2000.
41. **Dickens EJ, Edwards FR, and Hirst GD**. Selective knockout of intramuscular interstitial cells reveals their role in the generation of slow waves in mouse stomach. *J Physiol* 531: 827-833, 2001.
42. **Fox EA, Phillips RJ, Byerly MS, Baronowsky EA, Chi MM, and Powley TL**. Selective loss of vagal intramuscular mechanoreceptors in mice mutant for steel factor, the c-Kit receptor ligand. *Anat Embryol (Berl)* 205: 325-342, 2002.
43. **Horvath VJ, Vittal H, Lorincz A, Chen H, Almeida-Porada G, Redelman D, and Ordog T**. Reduced stem cell factor links smooth myopathy and loss of interstitial cells of cajal in murine diabetic gastroparesis. *Gastroenterology* 130: 759-770, 2006.
44. **Gibbons SJ, De Giorgio R, Faussone Pellegrini MS, Garrity-Park MM, Miller SM, Schmalz PF, Young-Fadok TM, Larson DW, Dozois EJ, Camilleri M, Stanghellini V, Szurszewski JH, and Farrugia G**. Apoptotic cell death of human interstitial cells of Cajal. *Neurogastroenterol Motil* 21: 85-93, 2009.
45. **Wouters MM, Gibbons SJ, Roeder JL, Distad M, Ou Y, Strege PR, Szurszewski JH, and Farrugia G**. Exogenous serotonin regulates proliferation of interstitial cells of Cajal in mouse jejunum through 5-HT2B receptors. *Gastroenterology* 133: 897-906, 2007.
46. **Choi KM, Gibbons SJ, Roeder JL, Lurken MS, Zhu J, Wouters MM, Miller SM, Szurszewski JH, and Farrugia G**. Regulation

of interstitial cells of Cajal in the mouse gastric body by neuronal nitric oxide. *Neurogastroenterol Motil* 19: 585–595, 2007.

47. **Young HM, Torihashi S, Ciampoli D, and Sanders KM.** Identification of neurons that express stem cell factor in the mouse small intestine. *Gastroenterology* 115: 898–908, 1998.
48. **Suzuki S, Suzuki H, Horiguchi K, Tsugawa H, Matsuzaki J, Takagi T, Shimojima N, and Hibi T.** Delayed gastric emptying and disruption of the interstitial cells of Cajal network after gastric ischaemia and reperfusion. *Neurogastroenterol Motil* 22: 585–593, e126, 2010.
49. **Choi KM, Gibbons SJ, Nguyen TV, Stoltz GJ, Lurken MS, Ordog T, Szurszewski JH, and Farrugia G.** Heme oxygenase–1 protects interstitial cells of Cajal from oxidative stress and reverses diabetic gastroparesis. *Gastroenterology* 135: 2055–2064, 2064 e2051–2052, 2008.
50. **Lefebvre RA, Dick JM, Guerin S, and Malbert CH.** Influence of the selective neuronal NO synthase inhibitor ARL 17477 on nitrergic neurotransmission in porcine stomach. *Eur J Pharmacol* 525: 143–149, 2005.
51. **McCloskey KD, Anderson UA, Davidson RA, Bayguinov YR, Sanders KM, and Ward SM.** Comparison of mechanical and electrical activity and interstitial cells of Cajal in urinary bladders from wild–type and W/Wv mice. *Br J Pharmacol* 156: 273–283, 2009.

국문 초록

노화에 따른 쥐 대장 근층의 지방 축적과 카할 간질세포 및 nNOS 양성 신경세포의 감소

서론: 대장에서 카할 간질세포의 노화에 따른 변화는 거의 알려진 바 없다. 본 연구의 목적은 노령 쥐 대장 근층의 형태학적 변화를 비롯하여 카할 간질세포 및 신경인성 일산화질소 합성효소(nNOS) 양성 신경세포의 노화에 따른 변화를 알아보는 것이다.

방법: 6 주령, 31 주령, 74 주령, 2 년령 F344 쥐의 근위부 대장을 실험에 이용하였다. C-Kit, nNOS 및 synaptophysin 면역화학염색을 통해 노화에 따른 카할 간질세포 및 대장 근층 내 신경의 수와 분포의 변화를 확인하였다. 또한 real-time PCR 을 이용하여 *C-kit, SCF*(stem cell factor)및 *nNOS* 의 mRNA 를 Western blot 실험을 통하여 c-Kit, nNOS 단백질을 각각 정량 하였다. 노화에 따른 기능적 변화를 알아보기 위해, 각 주령별로 등용성 근수축력을 측정하고 전기자극에 따른 근수축의 변화를 확인하였다.

결과: 근위부 대장 근육 내 지방 축적이 31 주령 이후, 노화에 따라 유의하게 증가하였다. 면역 염색 결과 c-Kit 양성 카할 간질세포 및 nNOS 양성 신경세포 및 신경섬유 역시 주령이 증가할수록 감소하는 양상을 보였다. c-kit 및 nNOS 의 mRNA 와 단백질도 주령이 증가하면서 감소하였다. 자발적 근수축력은 노령 쥐에서 감소하였으며, atropine 및 L-NG-Nitroarginine methyl ester 투여 후 전기자극에 대한 반응은 노령 쥐에서 모두 증가하는 양상을 보였다.

결론: 노령 쥐 대장 근층 내 지방 축적이 증가하고, 카할 간질 세포 및 nNOS 양성 신경세포및 신경섬유의 밀도가 감소하는 현상을 통해 노화로 인한 대장 운동 이상을 일부 설명할 수 있다.

주요어 : 노화, 대장, 카할 간질세포, 신경인성 일산화질소 합성효소, F344 쥐

학 번 : 2011-30579

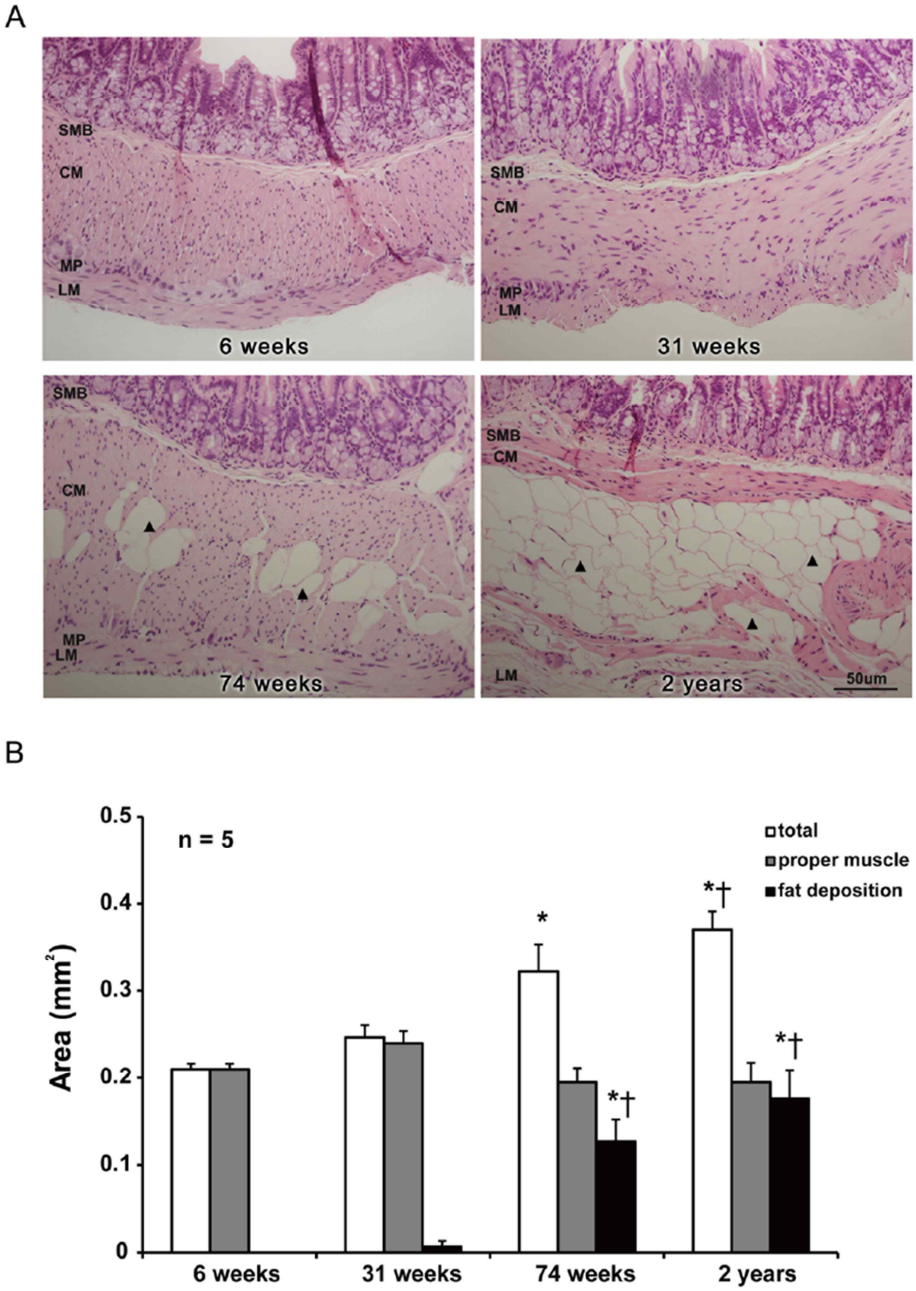

Fig. 1. The change of histology of tunica muscularis according to aging. *(A)* H&E stain (x 200 magnifications) and *(B)* statistical analysis for the measurement of each area. Total smooth muscle area and fat deposition (arrowhead) increased with age (P <0.001) but there was no

significant change in proper smooth muscle area ($P = 0.296$). Results are mean ± SE from 4to 6 animals per group. SMB, submucosal border; CM, circular muscle; MP, myenteric plexus; LM, longitudinal muscle. $^{*}P < 0.05$ compared with 6 weeks of age; $^{\dagger}P < 0.05$ compared with 31 weeks of age.

A

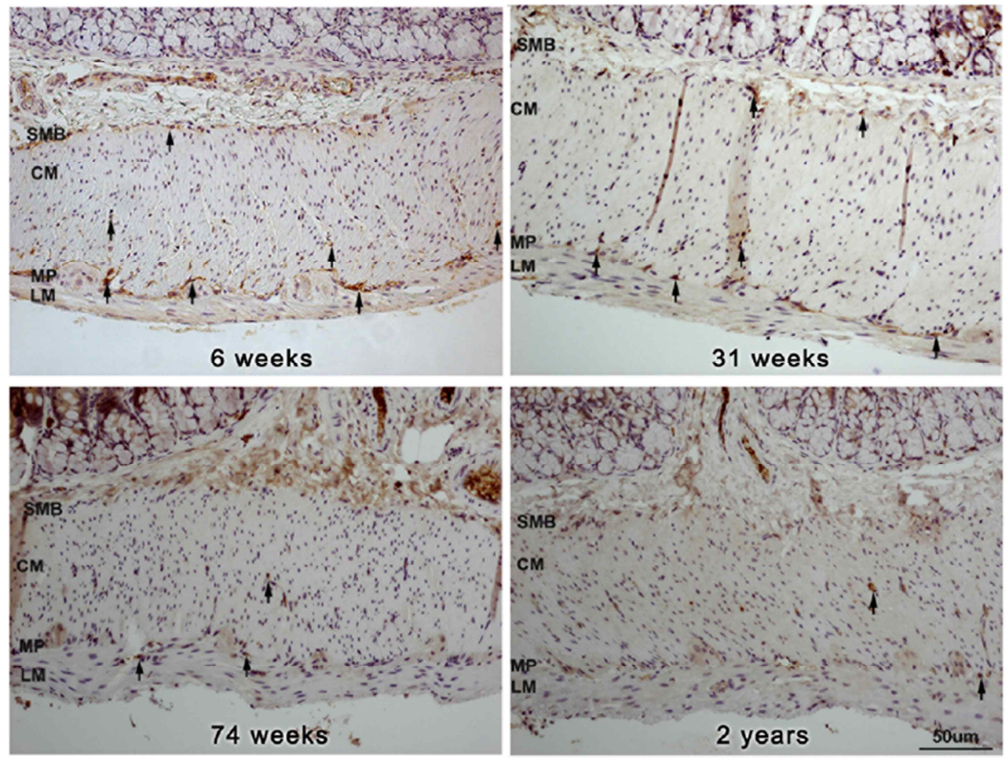
SMB
CM
MP
LM
6 weeks
SMB
CM
MP
LM
31 weeks
SMB
CM
MP
LM
74 weeks
SMB
CM
MP
LM
2 years
50um

B

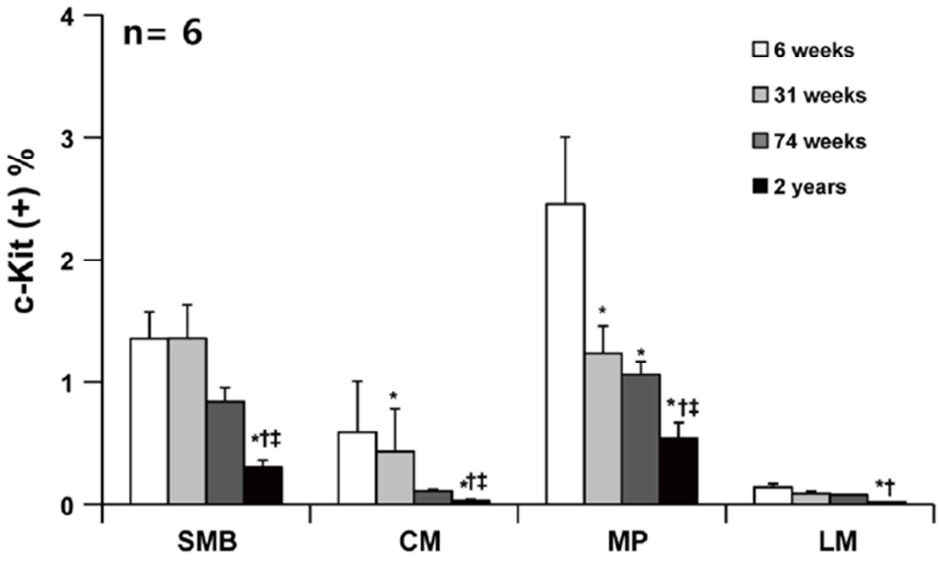
n= 6
c-Kit (+) %
4
3
2
1
0
6 weeks
31 weeks
74 weeks
2 years
*†‡
*
*†‡
*
*
*†‡
*†
SMB
CM
MP
LM

Fig. 2. Analysis of c-Kit immunohistochemistry. *(A)* Photomicrography of c-Kit immunostain of the proximal rat colon. Arrows indicate the c-Kit immunoreactive cell (x200 magnification). (*B*) The comparison of the proportion of c-Kit immunoreactivearea of SMB, MP, CM and LM in 6-, 31-, 74-weeks and 2-years-old rats (each group, $n = 6$). The proportion of c-Kit immunoreactive area showed the tendency to decrease with aging. The result was expressed as c-Kit positive percentage of total area of each region. Each bar represents the mean ± SE. SMB, submucosal border; MP, myenteric plexus; CM, circular muscle; LM, longitudinal muscle. $^{*}P < 0.05$ compared with 6-weeks of age; $^{\dagger}P < 0.05$ compared with 31 weeks of age; $^{\ddagger}P < 0.05$ compared with 74 weeks of age.

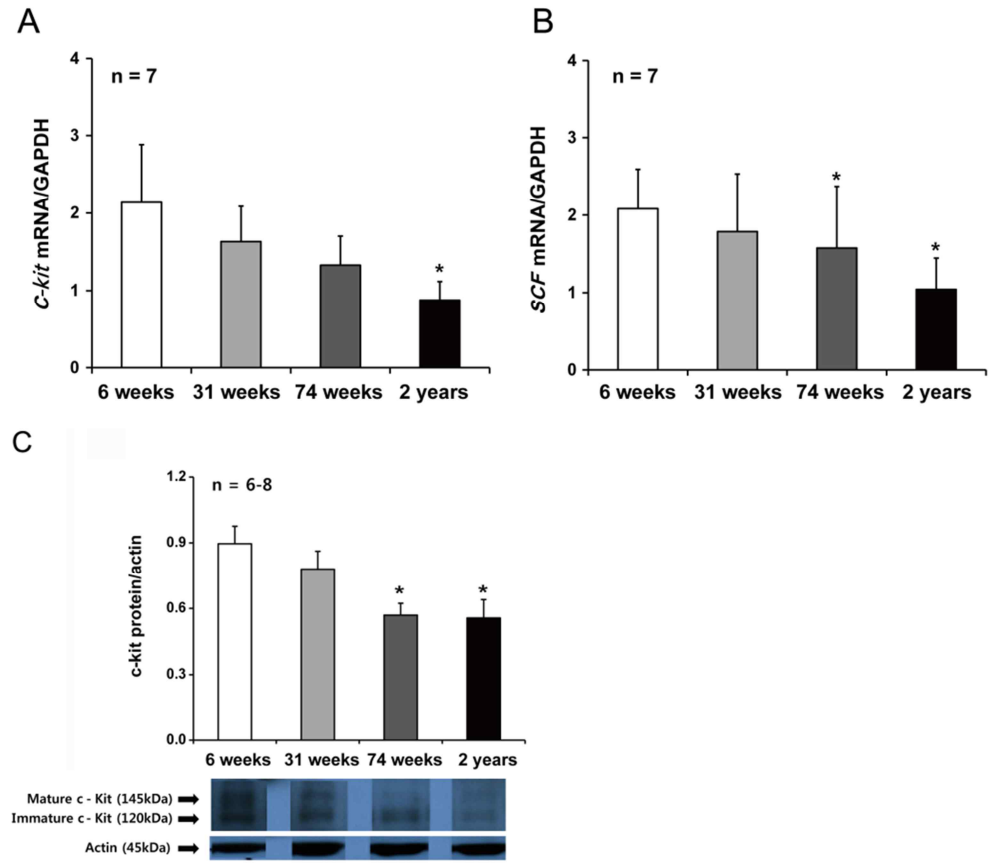

Fig. 3. The expression of *c-kit* mRNA, *SCF* mRNA and c-Kit protein. *(A)* The expression of *c-kit* mRNA by real-time PCR decreased with aging. That of 2-years-old rats significantly decreased compared to the 6-weeks-old rats ($P = 0.035$) (each group, n = 7). *(B) SCF* mRNA expression of 74-weeks and 2-years-old rats was significantly lower than that of 6-weeks-old rats ($P = 0.048$, $P = 0.002$, respectively) (each group, n = 7). *(C)* c-Kit protein expression decreased with aging. c-Kit protein expression of 74-weeks and 2-years old rats was lower than that of 6-weeks-old rats ($P = 0.015$ and $P = 0.029$, respectively) (n = 6 in 6-, 31- and 74 weeks, n=8 in 2 years). Results are shown as a mean value of the optical density (OD). Each of the optical density of mature (145 kDa) and immature (120 kDa) forms was combined into one in the analysis process using densirometry. Each bar represents the mean ± SE. $^{*}P < 0.05$ compared with 6-weeks of age.

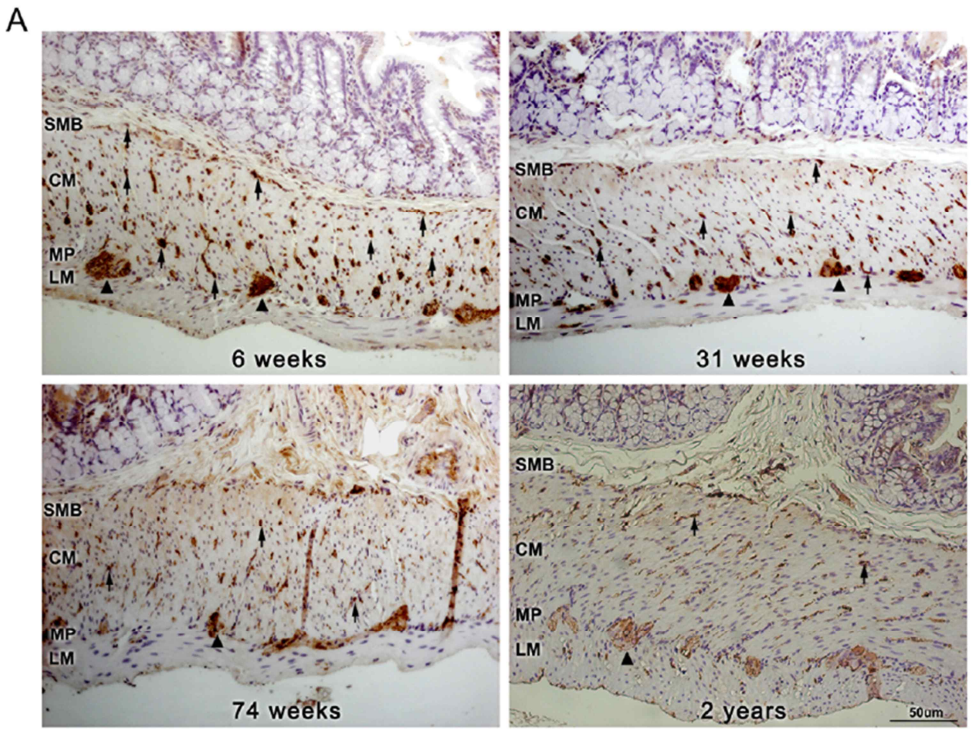
A
SMB
CM
MP
LM
6 weeks
SMB
CM
MP
LM
31 weeks
SMB
CM
MP
LM
74 weeks
SMB
CM
MP
LM
2 years
50um

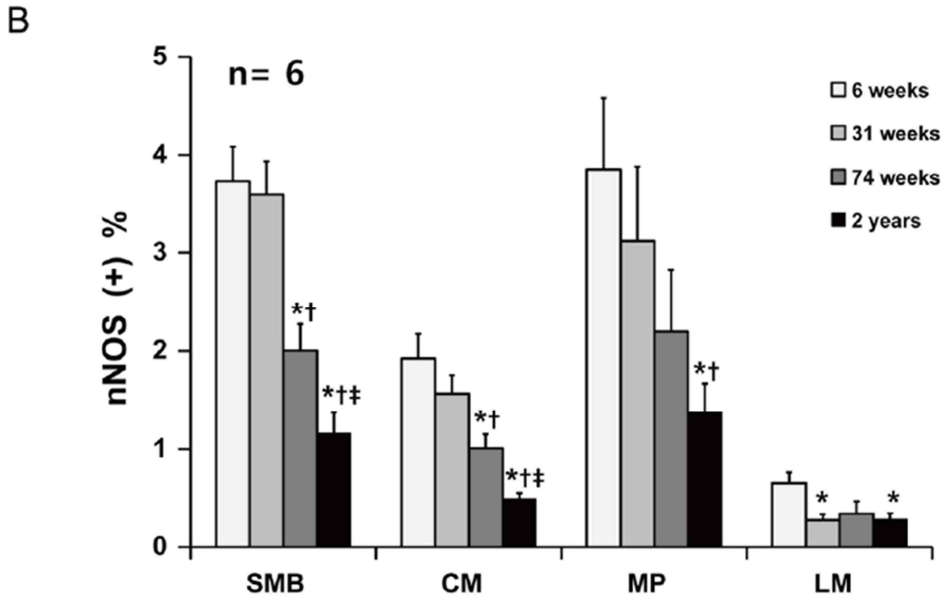
B
n= 6
6 weeks
31 weeks
74 weeks
2 years
nNOS (+) %
0
1
2
3
4
5
*†
*†‡
*†
*†‡
*†
*
*
SMB
CM
MP
LM

Fig. 4. Analysis of nNOS immunohistochemistry. *(A)* Photomicrography of nNOS immunostain of the proximal rat colon. Arrows and arrowheads indicate the nNOS positive nerve fibers and neuronal ganglion, respectively (x200 magnification). *(B)* The comparison of the nNOS positive area (each group, n = 6). The proportion of nNOS immunoreactive area showed the decreasing pattern with aging. Each bar represents the mean ± SE. SMB, submucosal border; MP, myenteric plexus; CM, circular muscle; LM, longitudinal muscle. $^{*}P < 0.05$ compared with 6-weeks of age; $^{\dagger}P < 0.05$ compared with 31 weeks of age; $^{\ddagger}P < 0.05$ compared with 74 weeks of age.

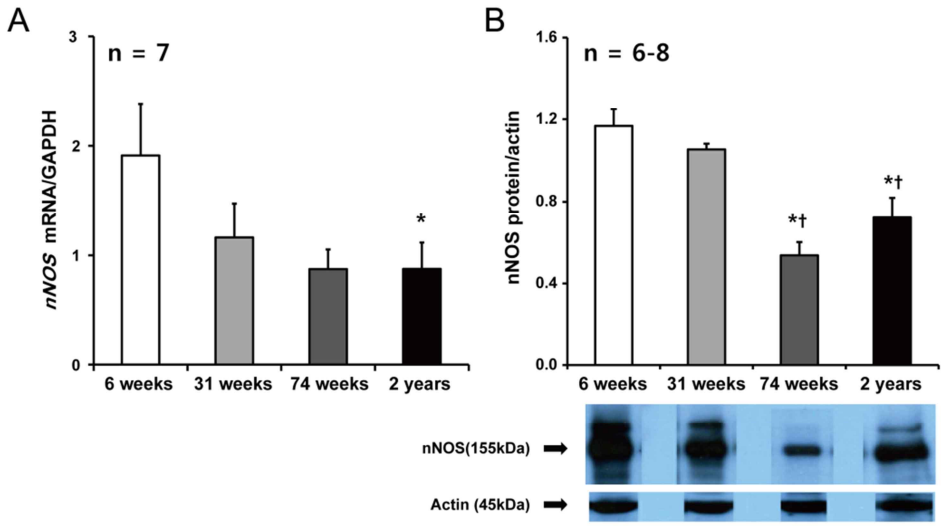

Fig. 5. The expression of *nNOS* mRNA and nNOS protein. *(A)* The expression of *nNOS* mRNA by real-time PCR decreased with aging. The expression of *nNOS* mRNA in 2-years-old rats was significantly lower than that of the 6-weeks-old rats ($P = 0.015$) (each group, n = 7). *(B)* nNOS protein expression on 74-weeks and 2-years-old rats showed significantly lower expression than that of the 6 and 31-wewks-old rats ($P < 0.001$ and $P = 0.003$ vs. 6 weeks, $P < 0.001$ and $P = 0.013$ vs. 31 weeks) (n = 6 in 6-, 31- and 74 weeks, n=8 in 2 years). Results are shown as a mean value of the optical density (OD). Each bar represents the mean ± SE. $^{*}P< 0.05$ compared with 6 weeks of age; $^{\dagger}P< 0.05$ compared with 31 weeks of age.

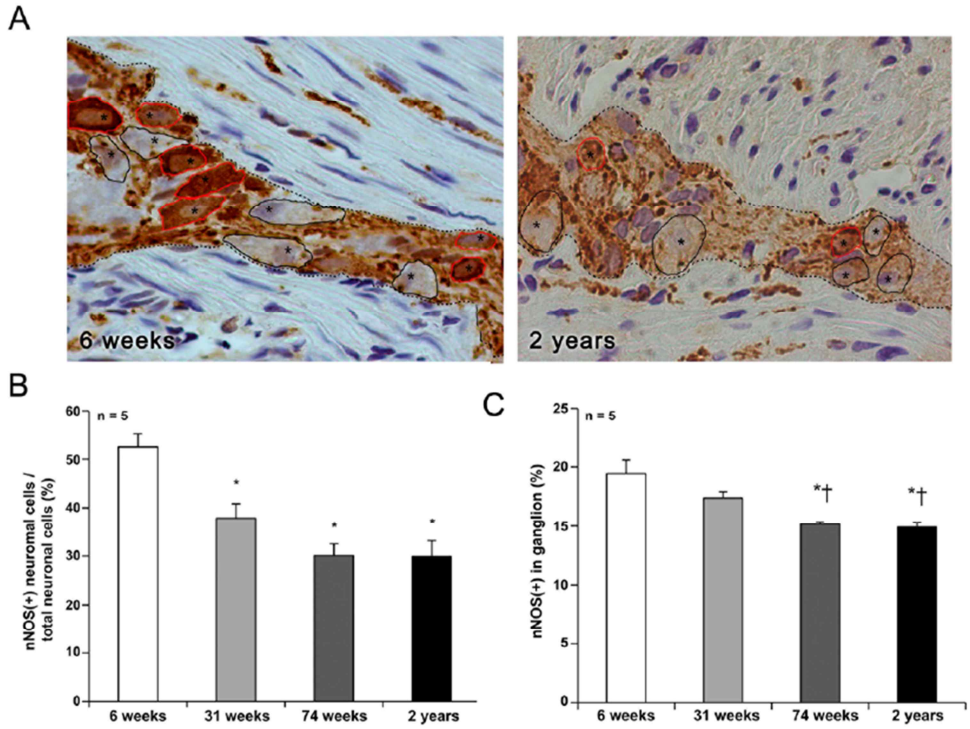

Fig. 6. The enumeration of neuronal cell in myenteric ganglia. *(A)* Ganglia in the myenteric plexus were micrographed at x1,000 (representative pictures of ganglion in 6-weeks and 2-years-old rat are shown). We enumerated the nNOS positive (indicated with red line) or negative (indicated with black line) myenteric neurons, which include nucleus (indicated with star), in the ganglion (contours of the ganglion are indicated by dotted lines). *(B)* The percent of nNOS positive neuronal cells of total neuronal cells in ganglionwas decreased with aging (P = 0.003). *(C)*The mean of proportion of nNOS immunoreactive area in ganglion was also decreased as age increased (P = 0.002). Each bar represents the mean ± SE. $^{*}P < 0.05$ compared with 6-weeks of age; $^{\dagger}P < 0.05$ compared with 31 weeks of age.

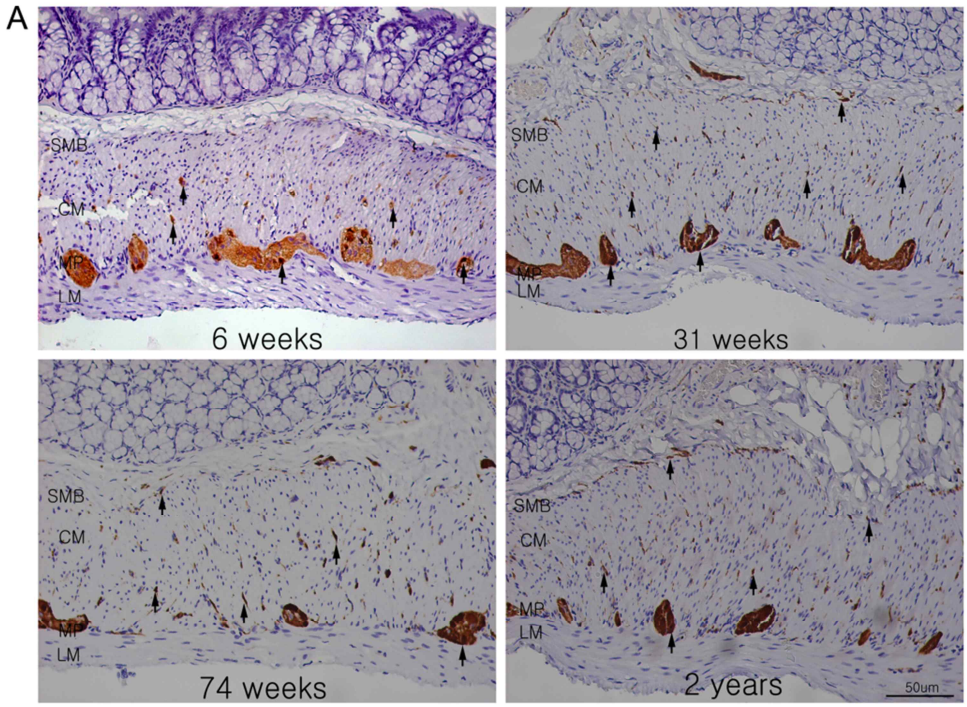
A
SMB
CM
MP
LM
6 weeks
31 weeks
74 weeks
2 years
50um

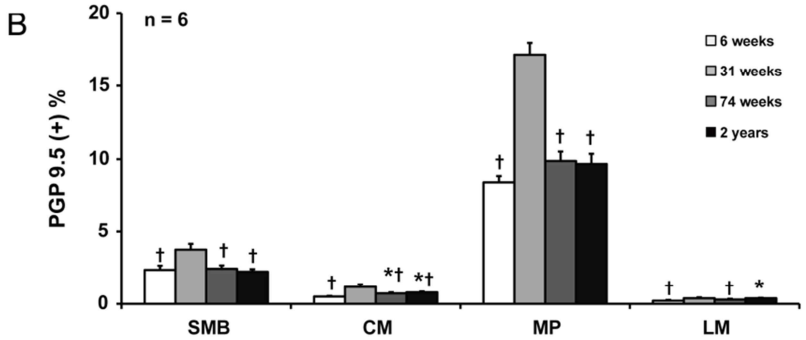
B
n = 6
PGP 9.5 (+) %
20
15
10
5
0
6 weeks
31 weeks
74 weeks
2 years
SMB
CM
MP
LM

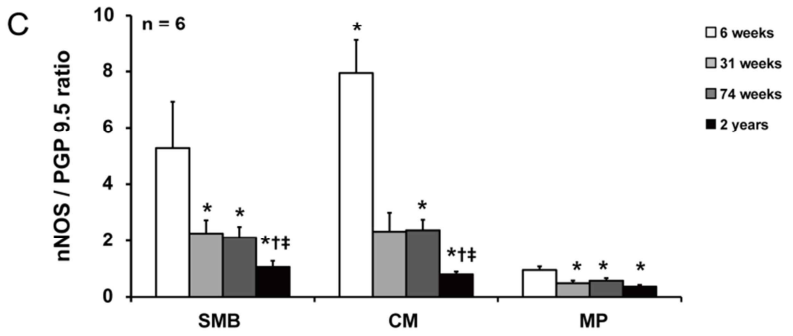
C
n = 6
nNOS / PGP 9.5 ratio
10
8
6
4
2
0
6 weeks
31 weeks
74 weeks
2 years
SMB
CM
MP

Fig. 7. Analysis of PGP 9.5 immunohistochemistry. *(A)* Photomicrography of PGP 9.5 immunostain of the proximal rat colon. Arrows indicate the PGP 9.5 immunoreactive nerve fibers and neuronal ganglion (x200 magnification). *(B)* The comparison of the PGP 9.5 positive area (each group, $n = 6$). The proportion of PGP 9.5 immunoreactive area showed the peak level in the 31-weeks-old rats and that of 74-weeks and 2-years-old rats decreased to the level of 6-weeks-old rats. *(C)* The comparison of ratio nNOS-positive area to PGP 9.5-positive area (each group, $n = 6$). 6-weeks-old rats showed the peak level with statistical significance and the relative ratio of nNOS/PGP 9.5 of 2-years-old rats was lower than that of other age groups (In SMB and CM, both $P < 0.001$ vs. 6 weeks, $P = 0.017$ and $P = 0.001$ vs. 31 weeks, $P = 0.004$ and $P < 0.001$ vs. 74 weeks; in MP, $P < 0.001$ vs. 6 weeks). The result was expressed as percentage of immunostain-positive area to total area of each region. Each bar represents the mean ± SE. SMB, submucosal border; MP, myenteric plexus; CM, circular muscle; LM, longitudinal muscle. $^{*}P < 0.05$ compared with 6-weeks of age; $^{\dagger}P < 0.05$ compared with 31 weeks of age; $^{\ddagger}P < 0.05$ compared with 74 weeks of age.

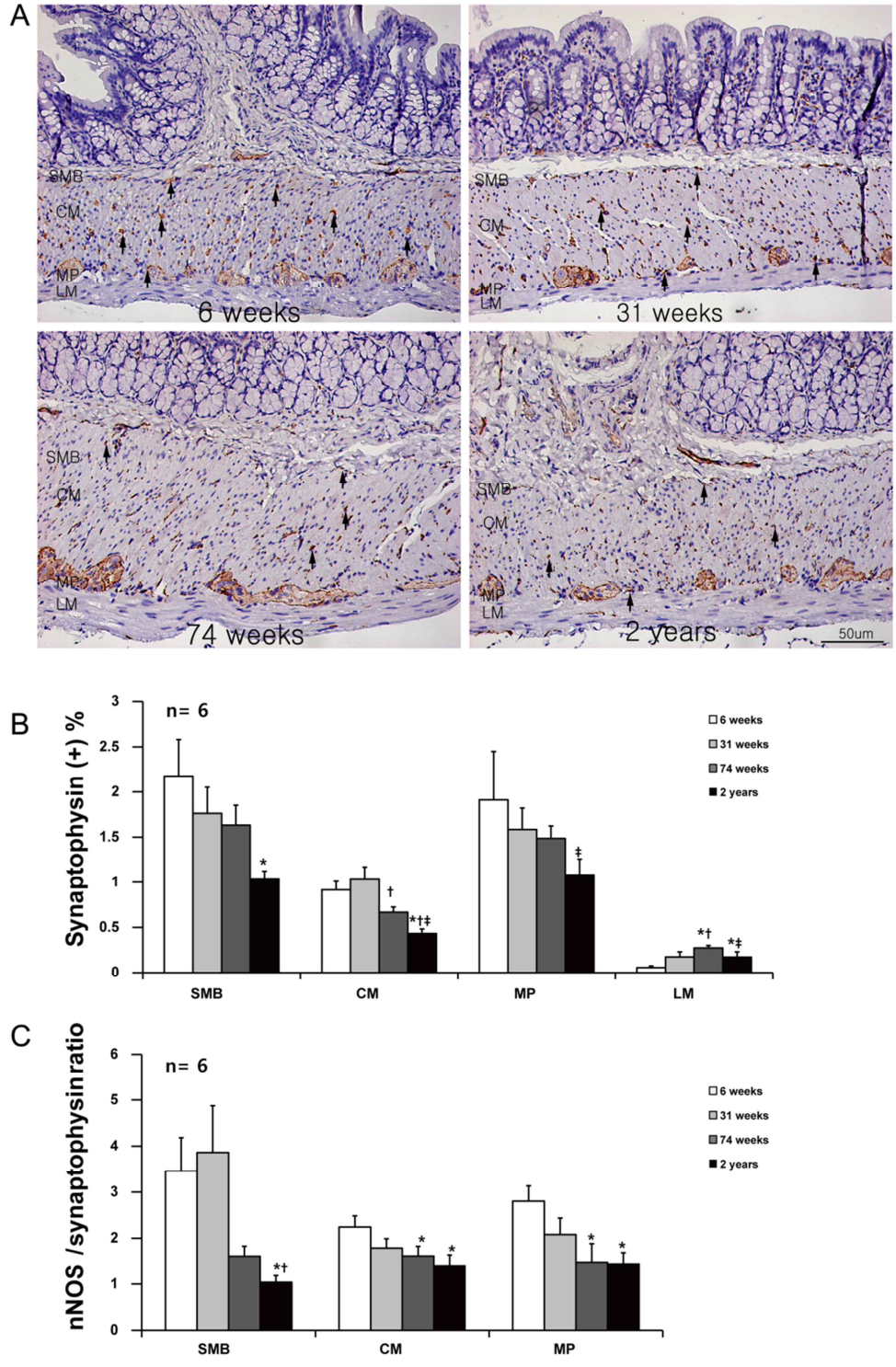
A
SMB
CM
MP
LM
6 weeks
31 weeks
74 weeks
2 years
50um
B
n= 6
Synaptophysin (+) %
6 weeks
31 weeks
74 weeks
2 years
SMB
CM
MP
LM
C
n= 6
nNOS /synaptophysinratio
SMB
CM
MP

Fig. 8. Analysis of synaptophysin immunohistochemistry. *(A)* Photomicrography of synaptophysin immunostain of the proximal rat colon. Arrows indicate the synaptophysin immunoreactive nerve fibers and neuronal ganglion (x200 magnification). (*B*) The comparison of the synaptophysin-positive area (each group, $n = 6$). (*C*) The comparison of ratio nNOS to synaptophysin-positive area (each group, $n = 6$). The result was expressed as percentage of immunostain-positive area to total area of each region. Each bar represents the mean ± SE. SMB, submucosal border; MP, myenteric plexus; CM, circular muscle; LM, longitudinal muscle. $^{*}P < 0.05$ compared with 6-weeks of age; $^{\dagger}P < 0.05$ compared with 31 weeks of age; $^{\ddagger}P < 0.05$ compared with 74 weeks of age.

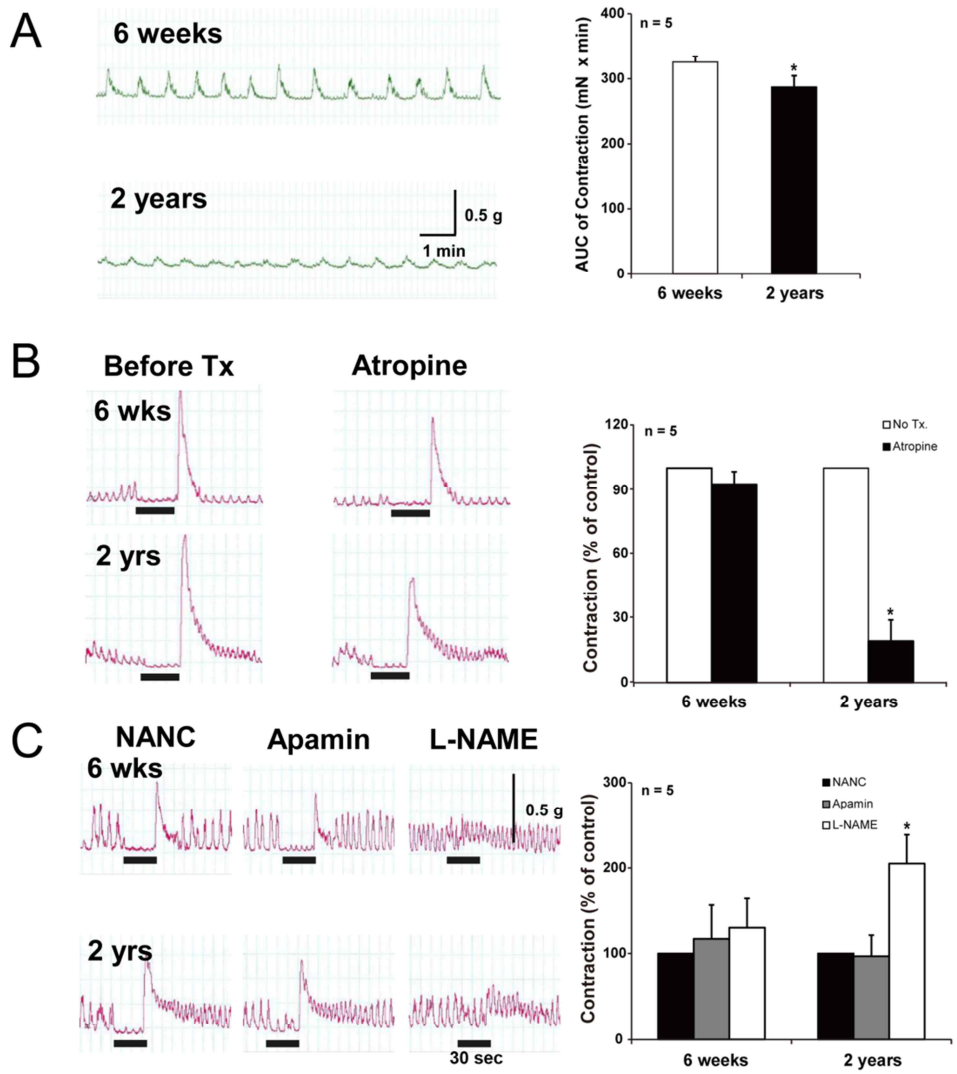

Fig. 9. Isovolumetric contractile measurement and electrical field stimulation. *(A)* The AUC of the spontaneous contractile response in resting state. The responses were significantly decreased in 2-years-old-rat colon (6-weeks-old rats 325.8 ± 8.9 vs. 2-years-old rats 287.2 ± 17.3 mN x min) ($P = 0.032$). $^{*}P < 0.05$ compared with 6 weeks of age. *(B)* The AUC of EFS during the contractile recordings. Colonic muscle contraction in 2-years-old rats was significantly inhibited by atropine

(10μM) (P = 0.000). $^{*}P < 0.05$ compared with no treatment. *(C)* The EFS responses of apamin and L-NAME under NANC condition. L-NAME (1μM) pretreatment significantly increased contractility in 2-years-old rats compared with the 6-weeks-old rats (P = 0.000). $^{*}P < 0.05$ compared with NANC condition. EFS, electrical field stimulation; NANC condition, non-adrenergic, non-cholinergic condition.

의학박사 학위논문

Fat deposition in the tunica muscularis and decrease of interstitial cells of Cajal (ICC) and nNOS positive neuronal cells in the aged rat colon

노화에 따른쥐 대장 근층의 지방 축적과 카할 간질세포 및 nNOS 양성 신경세포의 감소

2014년 2월

서울대학교 대학원
의학과 내과학전공
조 현 진

2014년 조 현 진

의학박사 학위논문

노화에 따른 쥐 대장 근층의 지방 축적과 카할 간질세포 및 nNOS 양성 신경세포의 감소

2014 년 2 월

서울대학교 대학원

의학과 내과학전공

조 현 진

A thesis of the Degree of Doctor of Philosophy

Fat deposition in the tunica muscularis and decrease of interstitial cells of Cajal (ICC) and nNOS positive neuronal cells in the aged rat colon

February 2014

The Department of Internal Medicine,

Seoul National University

College of Medicine

Hyun Jin Jo

노화에 따른 쥐 대장 근층의 지방 축적과 카할 간질세포 및 nNOS 양성 신경세포의 감소

Fat deposition in the tunica muscularis and decrease of interstitial cells of Cajal (ICC) and nNOS positive neuronal cells in the aged rat colon

지도교수 김 주 성

이 논문을 의학박사 학위논문으로 제출함

2013 년 10 월

서울대학교 대학원
의학과 내과학 전공

조 현 진

조현진의 의학박사 학위논문을 인준함

2014 년 2 월

위 원 장 정 현 채 (인)

부위원장 김 주 성 (인)

위 원 김 나 영 (인)

위 원 김 상 균 (인)

위 원 김 유 선 (인)

Fat deposition in the tunica muscularis and decrease of interstitial cells of Cajal (ICC) and nNOS positive neuronal cells in the aged rat colon

by
Hyun Jin Jo

A thesis submitted to the Department of Internal Medicine in partial fulfillment of the requirements for the Degree of Doctor of Philosophy in Internal Medicine at Seoul National University College of Medicine

February 2014

Approved by Thesis Committee:

Professor Hyun Chae Jung Chairman
Professor Joo Sung Kim Vice chairman
Professor Maxoung Kim
Professor Kang Gyun Kim
Professor You Sun Kim

ABSTRACT

Fat deposition in the tunica muscularis and decrease of interstitial cells of Cajal (ICC) and nNOS positive neuronal cells in the aged rat colon

Introduction: Little is known about the time-course of aging on interstitial cells of Cajal (ICC) of colon. The aim of this study was to investigate the change of morphology, ICC and neuronal nitric oxide synthase (nNOS) immunoreactive cells in the aged rat.

Methods: The proximal colon of 344 Fischer rats at four different ages (6, 31, 74 weeks, and 2 years) were studied. The immunoreactivity of c-Kit, nNOS, anti-protein gene product 9.5(PGP 9.5) and synaptophysin were counted after immunohistochemistry. The *c-kit*, *SCF* (stem cell factor; ligand of Kit) and *nNOS* mRNA were measured by real-time PCR. c-Kit and nNOS protein were assessed by Western blot.

Isovolumetric contractile force measurement and electrical field stimulation (EFS) were conducted.

Results: The area of intramuscular fat deposition significantly increased with age after 31 weeks. c-Kit immunoreactive ICC and nNOS immunoreactive neurons and nerve fibers significantly declined with age. mRNA and protein expression of c-kit and nNOS decreased with aging. The functional study showed that the spontaneous contractility was decreased in aged rat, whereas EFS responses to atropine and L-NG-Nitroarginine methyl ester were increased in aged rat.

Conclusions: In conclusion, the decrease of proportion of proper smooth muscle, the density of ICC and nNOS immunoreactive neuronal fibers and the number of nNOS immunoreactive neurons during the aging process may explain the aging-associated colonic dysmotility.

Keywords: aging, colon, Interstitial cells of Cajal, nNOS, Rats, Inbred F344

Student number: 2011-30579

CONTENTS

LIST OF FIGURES

LIST OF ABBREVIATIONS

ICC: interstitial cells of Cajal

nNOS: neuronal nitric oxide synthase

SCF: stem cell factor

EFS: electrical field stimulation

NO: nitric oxide

IHC: immunohistochemistry

H&E: hematoxylin and eosin

sGAG : sulfated glycosaminoglycan

LPO: lipid hydroperoxide

SMB: submucosal border

CM: circular muscle

MP: myenteric plexus

LM: longitudinal muscle

KRB: Krebs-Ringer bicarbonate

AUC: area under the curve

NANC: non-adrenergic non-cholinergic

Introduction

Aging leads to the impairment of organ function as a result of accumulation of diverse deleterious changes throughout the cells and tissues (1). Constipation is a common problem in the elderly and known to be associated with multiple factors, such as decreased intestinal secretory epithelial function, abnormal colonic motility caused by enteric neurodegeneration and reduced contractile response of smooth muscle cells with age (2-4).

Enteric neurodegeneration involves the loss of enteric neuron, especially, excitatory cholinergic neurons (5). In contrast, nitrergic myenteric neurons are known to be selectively spared in the aged (6-8). However, there was a contrary report that nitrergic neurons decreased in the aged rats (9). Nitrergic enteric neurons, which release nitric oxide (NO) generated by catalysis of neuronal nitric oxide synthase (nNOS), act as non-adrenergic, non-cholinergic inhibitory neuron and induce colonic smooth muscle relaxation (10). This NO is known to enhance transit of the rat colon by mediating descending relaxation, which in turn facilitates propulsion of the colonic

contents(11). Nitrergic nerves of colon may be an important component of colonic motility.

Interstitial cells of Cajal (ICC) also play important roles in gastrointestinal motility. ICC play as an electrical pacemaker as well as mediate both inhibitory and excitatory motor neurotransmissions which manifest as electrical slow waves in smooth muscles. Consequently, ICC contribute to segmenting and peristaltic contractile activity (12, 13). ICC have been diminished or lost in human disease for such as diabetic gastroenteropathy (14), slow transit constipation (15-17) and intestinal pseudo-obstruction (18). It is well known that ICC express proto-oncogene *c-kit* (19, 20). The stem cell factor (SCF) is natural ligand of Kit (21) and involves the development and maintenance of ICC (22). It has been known that the expression of *c-kit* mRNA and c-Kit protein significantly decreased in the colon of slow transit constipation patient and diabetes mellitus mouse (21, 23). In addition, there was a study on the number and volume of ICC networks in the normal human stomach and colon which declined with aging (24). In one study using progeric mouse, the percentage of ICC did not change and network volume of ICC decreased in the

proximal colon (25). However, a few data have been reported on the time-course of age related changes about ICC in the colon of conventional rats, so far. Furthermore, the results about age-related changes of nitrergic neurons are inconsistent. Previously, we reported that the lower part of rat gastric mucosa was replaced by connective tissue with accumulation of oxidative products with age (26). Similarly, we presumed a hypothesis that a certain morphologic change might occur in the colonic tissue with aging.

From this background, we aimed to assess the morphologic change and the changes of number and molecular expression of ICC, nNOS immunoreactive neurons and neuronal fibers in the proximal colon of rat at four different ages using immunohistochemistry (IHC) and molecular analysis.

Materials and Methods

Animals and tissue preparation.

Specific pathogen free, 344, male, Fischer rats (6-, 31-, 74-weeks and 2 years of age) were used (Orient Co. Ltd., Seoul, Korea). The animals were housed in a cage maintained at 23℃, with 12:12-hour light-dark cycles under specific pathogen-free conditions. The rats were starved but allowed for water for 12 hours prior to the experiments. The animals were anesthetized by zoletil and rompun mixture and killed by decapitation. One cm length of the proximal colon per each rat was obtained and fixed in 10% buffered formalin for histology. The specimens were embedded in paraffin and sectioned perpendicularly to the lumen (section thickness, 4 μm) and stained with hematoxylin and eosin (H&E). This study was approved by the Institutional Animal Care and Use Committee (IACUC) of Seoul National University Bundang Hospital.

Muscular histology.

The histology was evaluated by pathologist (H.S.L) blinded to

the age of the animal. The one H&E stained slide per rat (each age group, n = 5) and the two fields per slide were randomly selected. The area of the total smooth muscle, fatty tissue and proper muscle in the tunica muscularis of colon was quantified using the Image- Pro® Plus analysis system (Media Cybernetics, Inc., San Diego, CA, USA). The area was expressed as mm^2 per field of view.

Immunohistochemistry for c-Kit, nNOS, PGP(protein gene product)9.5 and synaptophysin.

For the c-Kit, nNOS, PGP 9.5 and synaptophysin IHC, the sections were incubated with the following primary antibody: anti-c-Kit antibody (dilution 1:100; polyclonal rabbit anti-human CD117, DAKO, Glostrup, Denmark), anti-nNOS antibody (dilution 1:500; AB5380 Chemicon, Millipore Corporation, Billerica, MA, USA), anti-PGP 9.5 antibody (dilution 1:250; CM 329 AK, Biocare Mecial, CA, USA) and anti-synaptophysin antibody (dilution 1:150; monoclonal mouse anti-human synaptophysin, clone SY38, DAKO, Glostrup, Denmark) after deactivation of endogenous peroxidase with 3% hydrogen peroxide and blocking of nonspecific binding sites. The

immunostain was performed using an automatic immunostainer (BenchMark XT, Ventana Medical Systems, Inc., Tucson, AZ, USA) according to the manufacturer's instructions. UltraView Universial DAB detection kit (Ventana Medical Systems) was used as secondary antibody. The negative control for IHC was performed without primary antibody.

The immunostained tissues were examined under a light microscope (Carl Zeiss, Jena, Germany) linked to a computer-assisted image analysis system (AxioVision Rel.4.8; Carl Zeiss). Two immunostained slides (one slide for synaptophysin) per each rat (each age group, n = 6) was made and four to five fields per slide were randomly selected and micrographed at x200. The micrograph was divided into four anatomic regions; submucosal border (SMB), circular muscle (CM), myenteric plexus (MP) and longitudinal muscle (LM) region (27) using Adobe photoshop ver. 7.0 (Adobe systems; Mountain View, CA, USA). Finally, quantitative assessment of c-Kit, nNOS, PGP 9.5 and synaptophysin immunoreactivity was performed using the Image- Pro® Plus analysis system and measurements were expressed as proportion of immunoreactive area (% of total area). Mast cells, which are known to express c-Kit but could

be identified by their round or oval shape and lack of processes, were excluded from the counts (14, 20, 24). Ganglia in the myenteric plexus were micrographed at x1000. The number of myenteric neurons, which include nucleus was enumerated.

Real-time PCR for c-kit, SCF and nNOS.

c-kit, *SCF* and *nNOS* mRNA were measured by real-time PCR (28). Briefly, RNA was extracted from the proximal colonic muscle tissues devoid of the mucosa, submucosa and preferably serosa using the RNeasy Plus Mini kit (Qiagen, Valencia, CA, USA) according to the manufacturer's instructions. RNA samples were diluted to a final concentration of 0.5 mg mL^{-1} in RNase-free water and stored at −80℃ until use. Synthesis of the cDNA was performed with 1 mg of total RNA with M-MLV reverse transcription reagents (Invitrogen, Carlsbad, CA, USA). The 20 μl reverse transcription reaction was consisted of 4 μl of first-strand buffer, 500 mM deoxynucleoside triphosphate mixture, 2.5 mM oligo(dT) 12-18 primer, 0.4 U mL^{-1}ribonuclease inhibitor, and 1.25 U mL^{-1}Moloney murine leukemia virus reverse transcriptase (Invitrogen). The thermal cycling parameters for the reverse transcription were 10

minutes at 65℃, 50 minutes at 37℃ and 15 minutes at 70℃. Real-time PCR amplification and determination were performed using SYBR Premix Ex TaqTM (Takara Bio, Shiga, Japan) according to manufacturer's protocols.

The following primers were used: *c-kit* forward, TTC CTG TGA CAG CTC AAA CG; *c-kit* reverse, AGC AAA TCT TCC AGG TCC AG; *SCF* forward, CAA AAC TGG TGG CGA ATC TT; *SCF* reverse, GCC ACG AGG TCA TCC ACT AT; *nNOS* forward, CTA CAA GGT CCG ATT CAA CAG; *nNOS* reverse, CCC ACA CAG AAG ACA TCA CAG; *GAPDH* forward, AGG TGA AGG TCG GAG TCA; and *GAPDH* reverse, GGT CAT TGA TGG CAA CAA. The *GAPDH* gene was used as an endogenous reference as a control for expression independent sample-to-sample variability. The amplification protocol consists of an initial denaturation step at 95℃ for 10 seconds followed by 40 cycles of denaturation for 5 seconds at 95℃ and annealing/extension of 33 seconds at 55℃. Relative expressions of target genes were normalized by dividing the target Ct values by the endogenous Ct values. All equipments were purchased from Applied Biosystems and used according to their protocols. RNA-free water was used in Real-time PCR as

no-template controls (NTC). After amplification, we performed melting curve analysis using ABI PRISM® 7000 Sequence Detection System software (Applied Biosystems).

Western blotting for c-Kit and nNOS.

The proximal colonic muscle tissue devoid of mucosa, submucosa and preferably serosa was homogenized with lysis buffer containing 25 mMTris-HCL (pH 7.4), EGTA (1 mM), DTT (1 mM), leupeptin (10 μg mL^{-1}), aprotinin (10 μg mL^{-1}), PMSF (1 mM), and Triton X-100 (0.1%). Briefly, the proteins (each sample, 100 μg) were separated by SDS-PAGE (8% wt/wt gel) and transferred to PVDF membranes. All procedures were performed in Tris buffer (40 mM, pH 7.55) containing 0.3 M of NaCl and 0.3% Tween 20. The membranes were then blocked with dried milk (5% wt/vol) and subsequently incubated with c-Kit (1:100; rabbit polyclonal antibody, Santa Cruz Biotechnology, Santa Cruz, CA, USA), nNOS (1:500; mouse monoclonal IgG2a antibody, BD Biosciences, San Diego, CA, USA) and β-actin (1:1000; rabbit polyclonal antibody, Biovision, Milpitas, CA, USA) at 4°C overnight. The blots were incubated with secondary antibody (rabbit polyclonal antibody, Santa Cruz

Biotechnology for c-Kit (dilution 1:500) and β-actin(dilution 1:1000), mouse polyclonal antibody, 1:1000; Santa Cruz Biotechnology for nNOS) and an imaging analyzer was used to measure the band densities. For c-Kit immunoblot, each of the optical density of mature (145 kDa) and immature (120 kDa) forms was combined into one in the analysis process using densirometry(29).

Isometric force measurements and electrical field stimulation.

Mechanical responses were performed to investigate the functional difference of colon between 6- weeks and 2-years-old F344 rats using standard organ-bath techniques. Segments of the proximal colon were removed through a midline abdominal incision and opened along the mesenteric border. Luminal contents were removed by washing with Krebs–Ringer bicarbonate solution (KRB), and the mucosa was removed leaving the tunica muscularis and remnants of the submucosa. The muscles were mounted under 1 g tension and then allowed to equilibrate for 1–2 hours with constant perfusion with fresh KRB. The spontaneous contractile activity was measured by

area under the curve (AUC) at the resting state and then electrical field stimulation (EFS, 5 Hz, 320 mA, 1 ms for 30 seconds) was performed to induce neural response with parallel platinum wire electrodes to colonic muscle strips. The contraction and relaxation responses by EFS of colonic muscle were measured under atropine (10 μM) sequentially. And the EFS responses to apamin (1 μM) and L-NG-Nitroarginine methyl ester (L-NAME, 10 μM) were determined under non-adrenergic non-cholinergic (NANC) condition by adding atropine, propranolol, and phentolamine (each 1 μM). All data were recorded using the PowerLab data acquisition system. Using the recorded waveform, the AUC was calculated by integrating the differences between the maximum and minimum values obtained immediately before and after the EFS stimulation. When measuring the percent changes of EFS response under drug pretreatment, the value before the drug treatment was defined as 100%.

Statistical analysis.

All statistical calculations were performed using SPSS software (version 18.0; SPSS Inc., Chicago, IL, USA). The

results were compared by the Mann-Whitney U-test and the Wilcoxon's rank-sum test. All values are reported as means ± SE. A $P < 0.05$ was considered statistically significant.

Results

Influence of aging on intramuscular fat deposition.

The total area of tunica muscularis of the proximal colon significantly increased with age (Fig. 1). However, most of this increase was originated from the deposition of intramuscular fat with age ($P < 0.001$) (Fig. 1). There was no fat deposition in 6-week, but observed only in one field in 31-weeks-old. However, fat deposition was observed in all fields of 74-weeks-old and 2-years-old rat. There was no significant change in proper smooth muscle area ($P = 0.296$).

Influence of aging on ICC.

The proportion of c-Kit-positive area decreased with aging. That of 2-years-old rat was significantly decreased compared to 6-, 31- and 74-weeks-old rat in SMB, CM and MP (SMB, $P < 0.001$ vs. 6 and 31 weeks, $P = 0.013$ vs. 74 weeks; CM, $P < 0.001$ vs. 6 and 31 weeks, $P = 0.002$ vs. 74 weeks; MP, $P < 0.001$ vs. 6 weeks, $P = 0.001$ vs. 31 weeks, $P = 0.003$ vs. 74 weeks). Also, the proportion of c-Kit-positive area of 31-

weeks and 74-weeks-old rat was significantly lower than that of 6-weeks-old rats in all area (31 weeks, P = 0.046, P = 0.019, P = 0.007 and P = 0.007; 74 weeks, all P < 0.001 in SMB, CM, MP and LM) (Fig. 2).

c-kit mRNA expression decreased with aging. That of 2-years-old rats significantly decreased compared to the 6-weeks-old rats (P = 0.035) (Fig. 3*A*). Similarly, *SCF* mRNA expression of 74-weeks and 2-years-old rats was significantly lower than that of 6-weeks-old rats (P = 0.048, P = 0.002, respectively) (Fig. 3*B*). c-Kit protein expression was the highest in 6-weeks-old rats and decreased with aging. c-Kit protein expression of 74-weeks and 2-years old rats was significantly lower than that of 6-weeks-old rats (P = 0.015 and P = 0.029, respectively) (Fig. 3*C*).

Influence of aging on nNOS positive neurons and immunoreactivity of PGP 9.5 and synaptophysin .

Similar to c-Kit immunostain, a larger proportion of nNOS-positive area was present in the 6 weeks old and it rapidly decreased with age (Fig. 4*A*) In SMB, CM and MP, the proportion of nNOS-positive area of 2-years-old rats was

significantly lower than that of 6-, 31- and 74-weeks-old rats (SMB and CM, all $P < 0.001$; MP, $P = 0.002$, $P = 0.004$ and $P = 0.027$).That of 74-weeks-old rats was significantly lower compared to 6- and 31-weeks-old rats in SMB ($P < 0.001$and $P = 0.015$, respectively). For CM and LM, nNOS-positive area of 31- and 74 weeks-old rats was lower than that of 6-weeks-old rats with statistical significance (CM, both $P < 0.001$; LM, $P = 0.002$ and $P = 0.013$) (Fig. 4*B*). In terms of *nNOS* mRNA expression, 2-years-old rats showed significant decrease compared to the 6-weeks-old rats ($P = 0.015$) (Fig. 5*A*). nNOS protein expression was lower in 74-weeks and 2-years-old rats than that of the 6- and 31-weeks-old rats and there was statistical significance (In 74 weeks, all $P < 0.001$; In 2 years, $P = 0.003$ vs. 6 weeks, $P = 0.013$ vs. 31 weeks) (Fig. 5*B*).

When myenteric ganglion was analyzed (Fig. 6*A*), the percent of nNOS-positive neuronal cell per total neuronal cell was also decreased as age increased (Fig. 6*B*). The proportion of nNOS-immunoreactive area of 74-weeks and 2-years-old rats were also significantly lower than 6- and 31-weeks-old rats (Fig. 6*C*).

PGP 9.5 immuno-positive area of 31-weeks-old rats was most high compared to other age groups in SMB, CM, MP and LM. PGP 9.5 immuoreactivity of 74-weeks and 2-years old rats was similar or slightly higher than 6-weeks-old rats (Fig 7*A* and 7*B*). However, for the relative ratio of nNOS-positive area to PGP 9.5-positive area, 6-weeks-old rats showed the peak level with statistical significance and the relative ratio of nNOS/PGP 9.5 of 2-years-old rats was lower than that of other age groups (In SMB and CM, both $P < 0.001$ vs. 6 weeks, $P = 0.017$ and $P = 0.001$ vs. 31 weeks, $P = 0.004$ and $P < 0.001$ vs. 74 weeks; in MP, $P < 0.001$ vs. 6 weeks) (Fig 7*C*).

The proportion of synaptophysin-positive area generally tended to decrease with age except LM (Fig. 8*A* and 8*B*) and the ratio of nNOS-positive area to synaptophysin-positive area was also significantly lower in the aged rats compared to young rats (Fig. 8*C*). The proportion of synaptophysin-positive area of 2-years-old rats was significantly lower than that of 6-weeks-old rats in SMB ($P = 0.016$) and 74-weeks-old rats in MP ($P = 0.015$). In CM, the proportion of synaptophysin-positive area of 2-years-old rat was significantly decreased compared with other groups ($P < 0.001$ compared to 6 weeks

and 31 weeks, and P = 0.005 compared to 74 weeks). In addition, the ratio of nNOS to synaptophysin of 74−weeks and 2−years−old rats was decreased compared to 6−weeks−old rats in CM (P = 0.044 in 74weeks, P = 0.008 in 2 years) and MP (P = 0.003 in 74 weeks, P = 0.011 in 2 years). In SMB, the ratio of nNOS to synaptophysin of 2−years−old rats was lower than that of 6−weeks and 31−weeks−old rats (P = 0.004 to 6 weeks, P < 0.001 to 31 weeks). As there were cases that the value of nNOS, PGP 9.5 or synatophysin−positive area was zero in LM, the statistical analysis was not performed in LM.

Influence of aging on colonic motility.

The AUC of colonic spontaneous contraction in 2−years−old rats, measured by isometric force measurement, was significantly decreased compared with the 6−weeks−old rats (6−weeks−old, 325.8 ± 8.9 mN x min vs. 2−years−old, 287.2 ± 17.3 mN x min) (P = 0.032) (Fig. 9*A*). The contractile response to EFS of 2−years−old rats was significantly inhibited by atropine compared with the 6−weeks−old rats (6−weeks−old, 92.5±5.9 % vs. 2−years−old, 19.2 ± 9.7) (P = 0.000) (Fig. 9*B*). Under the NANC condition, apamin

pretreatment did not affect the response to EFS in both aged rat colon (6-weeks-old, 116.9±40.2 % vs. 2-years-old, 97.0 ±24.4), however L-NAME pretreatment significantly increased contractility in 2-years-old rats compared with the 6-weeks-old rats (6-weeks-old, 129.8±35.0 % vs. 2-years-old, 205.1±33.7) (P = 0.000) (Fig. 9*C*).

Discussion

When we assessed the morphologic and molecular changes of ICC and nNOS-positive enteric neurons in the rat colon using four different age groups of 344 Fischer rats, the most peculiar finding was thickening of muscular layer with age, which was originated from fat deposit. These changes have not been reported in human as well as experimental animals, so far. The mechanism of fat deposition in colonic smooth muscle of rat including oxidative stress and its effects on the contraction are needed to be investigated in the future.

Several studies demonstrated that the number of myenteric neurons of the rat colon decreased with aging (30). However, the loss of enteric neurons was mainly cholinergic neurons, and nNOS-positive nitrergic neurons were known to be relatively spared (5, 6, 30-32). In the preset study, the relative ratio of nNOS/PGP 9.5 immunoreactivity and the percent of nNOS-positive neuronal cell per total neuronal cell were analyzed to exclude the dilution effect by growth. The result clearly showed the decrease of nNOS-immunoreactive neuronal cells

with age, which might be related to the damage of nitrergic neurons, such as axonal swelling and loss of expression of NOS in aged rats (7, 9). Similarly, aging gastric mucosa has shown reduced nNOS activity (26, 33). The decrease of nNOS-positivity was found to be originated from the selective loss of nNOS neurons. Even though this result could not completely exclude the possibility of loss of nNOS enzyme expression with aging, the decrease of relative ratio of nNOS/PGP 9.5-immunoreactivity together with the decline of the percent of nNOS-positive neuronal cell per total neuronal cell might suggest the loss of nitrergic neurons in the old aged rats.

The ICC are necessary for maintaining gastrointestinal motility. The decrease of ICC, as observed in several motility disorders (14-16, 18, 34, 35), reduces amplitudes of slow wave, consequently, induces intestinal dysmotility by reducing electrical drive to smooth muscle contractions and peristalsis (36). Recent study has shown that the number and volume of ICC networks in the normal human stomach and colon declined with age using IHC analysis but related molecular analysis, such as Western immunoblotting or real-time PCR, was absent in that study (24). Similarly, the ICC network volumes were

reduced in proximal colon of progeric mice, but little is known about the time course of age-related changes on ICC in conventional rat model (23, 28). In the present study the proportion of c-Kit-positive area, the largest of which located at the region of the MP, clearly decreased with aging. This depletion of c-Kit-positive ICC was diffuse across the layers of the rat colon. As ICC is an important factor of gastrointestinal motility, the diffuse reduction of density of ICC with age may explain the aging-associated colonic dysmotility.

The SCF/*c-kit* signal pathway is critical in the normal development, maturation, and phenotype maintenance of ICC (37-40). The primary loss of intramuscular ICC and reduction in myenteric ICC were noted not only in *kit* mutant mice (W/W^V) (41) but also in SCF mutant Sl/Sl^d mice (42). However, the underlying mechanism for the decrease of ICC with age is not well known yet. Recent study on the stomach of progeric mice suggested that the loss of ICC with age was dependent on multiple factors such as reduction in SCF, low circulating insulin and IGF-I levels and increased oxidative stress (31). In the present study, the expression of *c-kit* mRNA and c-Kit protein was decreased with aging. Another molecular work in the

present study, *SCF* mRNA also showed a good correlation of decreasing pattern with the c-Kit protein and *c-kit* mRNA expression. These results together with the previous reports (21, 40, 43) suggest that the SCF preferentially contributes to expression of c-Kit-positive ICC.

In addition to activation of the c-kit receptor via SCF, the release of neuronal nitric oxide is also known to increase proliferation of ICC in mice (44, 45). In the study using stomach body tissue of mouse, ICC volume and c-Kit protein of neuronal $NOS^{-/-}$ mouse were decreased than control. Additionally, number of ICC in primary cell culture and organotypic culture were increased by nitric oxide donor (46). Furthermore, there was a report that nitrergic enteric neurons act as a source of SCF (47). In the present study, nNOS-positive neurons and neuronal fibers of the rat proximal colon as well as the expression of nNOS protein decreased with age. Similarly, the *nNOS* mRNA of 2-years-old rats was significantly lower than that of 6-weeks-old rats. Since the nNOS-derived NO is important for the presence of ICC in the gastrointestinal tract (48), the loss of nNOS-positive neuronal

cells in the aged rat colon might cause adverse effect on ICC maintenance.

There are also other evidences that oxidative stress may induce loss of ICC or nNOS. For example, Klotho-deficient progeric mice showed profound ICC loss, but Klotho protected ICC by limiting oxidative stress (31). In addition, c-Kit and nNOS expressions were lost during diabetic gastroparesis due to increased levels of oxidative stress caused by low levels of heme oxygenase-1, an important cytoprotective molecule against oxidative injury (49). We detected that colonic mucosal LPO, although it was measured in the mucosa (data was not shown), increased during the aging process. Taken together the decrease of density of ICC and nNOS in the rat colon with aging also could be a consequence of oxidative stress.

EFS for evaluation of functional difference between 6-weeks and 2-years old rats showed that spontaneous colonic muscle contraction at resting state significantly decreased in the aged rat , although the difference between two age groups was very small (Fig. 9*A*). The decreased spontaneous activities in 2-years-old rats might be affected by both the damage of ICC and the degeneration of enteric neuron with aging. The

response to EFS under the treatment of atropine (Fig. 9*B*) or L-NAME (Fig. 9*C*) was different between two age groups. Both the relative decline of contractile response to EFS under the atropine pretreatment and the relative increment of contractile response to EFS under the L-NAME were significantly larger in aged rats compared with young rats (Fig. 9*B* and 9*C*). It is well known that atropine and L-NAME inhibit the action of excitatory cholinergic and inhibitory nitrergic neuron, respectively (50, 51). Therefore, it would be possible that the relatively increased response to atropine and L-NAME in the aged rats could reflect the degeneration of cholinergic and nitrergic neuron, respectively. However, this explanation needs further experiment.

We used the image analyzer to quantify ICC and nNOS-positive neuronal structures. This method offered several advantages over conventional cell counting techniques. That is, it allowed cell density to be determined in areas with difficulty in identifying individual cells due to high density. The strong point of this study is that we showed the age-related changes of density and molecular expression of ICC and nNOS-positive enteric neurons in the rat colon in four different ages using IHC

study together with molecular analysis. In conclusion, the proportion of proper smooth muscle in the tunica muscularis, the density of ICC and nNOS-immunoreactive neuronal fibers and the number of nNOS-immunoreactive neurons were decreased during the aging process in the proximal colon of rat. This change might cause impairment of colonic smooth muscle contraction and could be one mechanism for constipation in the elderly. Additional functional and physiologic study, which might provide a direct relationship, is currently underway.

References

1. **Harman D.** Aging: overview. *Ann N Y Acad Sci* 928: 1-21, 2001.
2. **Bitar KN, and Patil SB.** Aging and gastrointestinal smooth muscle. *Mech Ageing Dev* 125: 907-910, 2004.
3. **Braaten B, Madara JL, and Donowitz M.** Age-related loss of nongoblet crypt cells parallels decreased secretion in rabbit descending colon. *Am J Physiol* 255: G72-84, 1988.
4. **Camilleri M, Cowen T, and Koch TR.** Enteric neurodegeneration in ageing. *Neurogastroenterol Motil* 20: 418-429, 2008.
5. **Bernard CE, Gibbons SJ, Gomez-Pinilla PJ, Lurken MS, Schmalz PF, Roeder JL, Linden D, Cima RR, Dozois EJ, Larson DW, Camilleri M, Zinsmeister AR, Pozo MJ, Hicks GA, and Farrugia G.** Effect of age on the enteric nervous system of the human colon. *Neurogastroenterol Motil* 21: 746-e746, 2009.
6. **Cowen T, Johnson RJ, Soubeyre V, and Santer RM.** Restricted diet rescues rat enteric motor neurones from age related cell death. *Gut* 47: 653-660, 2000.
7. **Phillips RJ, Kieffer EJ, and Powley TL.** Aging of the myenteric plexus: neuronal loss is specific to cholinergic neurons. *Auton Neurosci* 106: 69-83, 2003.
8. **Wade PR, and Cowen T.** Neurodegeneration: a key factor in the ageing gut. *Neurogastroenterol Motil* 16 Suppl 1: 19-23, 2004.
9. **Takahashi T, Qoubaitary A, Owyang C, and Wiley JW.** Decreased expression of nitric oxide synthase in the colonic myenteric plexus of aged rats. *Brain Res* 883: 15-21, 2000.

10. **Takahashi T, and Owyang C.** Regional differences in the nitrergic innervation between the proximal and the distal colon in rats. *Gastroenterology* 115: 1504-1512, 1998.
11. **Mizuta Y, Takahashi T, and Owyang C.** Nitrergic regulation of colonic transit in rats. *Am J Physiol* 277: G275-279, 1999.
12. **Huizinga JD.** Gastrointestinal peristalsis: joint action of enteric nerves, smooth muscle, and interstitial cells of Cajal. *Microsc Res Tech* 47: 239-247, 1999.
13. **Nakagawa T, Misawa H, Nakajima Y, and Takaki M.** Absence of peristalsis in the ileum of W/W(V) mutant mice that are selectively deficient in myenteric interstitial cells of Cajal. *J Smooth Muscle Res* 41: 141-151, 2005.
14. **Nakahara M, Isozaki K, Hirota S, Vanderwinden JM, Takakura R, Kinoshita K, Miyagawa J, Chen H, Miyazaki Y, Kiyohara T, Shinomura Y, and Matsuzawa Y.** Deficiency of KIT-positive cells in the colon of patients with diabetes mellitus. J Gastroenterol Hepatol 17: 666-670, 2002.
15. **Geramizadeh B, Hayati K, Rahsaz M, and Hosseini SV.** Assessing the interstitial cells of Cajal, cells of enteric nervous system and neurotransmitters in slow transit constipation, using immunohistochemistry for CD117, PGP9.5 and serotonin. *Hepatogastroenterology* 56: 1670-1674, 2009.
16. **He CL, Burgart L, Wang L, Pemberton J, Young-Fadok T, Szurszewski J, and Farrugia G.** Decreased interstitial cell of cajal volume in patients with slow-transit constipation. *Gastroenterology* 118: 14-21, 2000.
17. **Lee JI, Park H, Kamm MA, and Talbot IC.** Decreased density of interstitial cells of Cajal and neuronal cells in patients

with slow-transit constipation and acquired megacolon. *J Gastroenterol Hepatol* 20: 1292-1298, 2005.

18. **Isozaki K, Hirota S, Miyagawa J, Taniguchi M, Shinomura Y, and Matsuzawa Y.** Deficiency of c-kit+ cells in patients with a myopathic form of chronic idiopathic intestinal pseudo-obstruction. *Am J Gastroenterol* 92: 332-334, 1997.
19. **Chen H, Redelman D, Ro S, Ward SM, Ordog T, and Sanders KM.** Selective labeling and isolation of functional classes of interstitial cells of Cajal of human and murine small intestine. *Am J Physiol Cell Physiol* 292: C497-507, 2007.
20. **Ward SM, and Sanders KM.** Physiology and pathophysiology of the interstitial cell of Cajal: from bench to bedside. I. Functional development and plasticity of interstitial cells of Cajal networks. *Am J Physiol Gastrointest Liver Physiol* 281: G602-611, 2001.
21. **Yamamoto T, Watabe K, Nakahara M, Ogiyama H, Kiyohara T, Tsutsui S, Tamura S, Shinomura Y, and Hayashi N.** Disturbed gastrointestinal motility and decreased interstitial cells of Cajal in diabetic db/db mice. *J Gastroenterol Hepatol* 23: 660-667, 2008.
22. **Ordog T, Hayashi Y, and Gibbons SJ.** Cellular pathogenesis of diabetic gastroenteropathy. *Minerva Gastroenterol Dietol* 55: 315-343, 2009.
23. **Tong WD, Liu BH, Zhang LY, Xiong RP, Liu P, and Zhang SB.** Expression of c-kit messenger ribonucleic acid and c-kit protein in sigmoid colon of patients with slow transit constipation. *Int J Colorectal Dis* 20: 363-367, 2005.
24. **Gomez-Pinilla PJ, Gibbons SJ, Sarr MG, Kendrick ML, Shen KR, Cima RR, Dozois EJ, Larson DW, Ordog T, Pozo MJ, and Farrugia G.** Changes in interstitial cells of cajal with age in the human stomach and colon. *Neurogastroenterol Motil* 23: 36-44, 2011.

25. Asuzu DT, Hayashi Y, Izbeki F, Popko LN, Young DL, Bardsley MR, Lorincz A, Kuro OM, Linden DR, Farrugia G, and Ordog T. Generalized neuromuscular hypoplasia, reduced smooth muscle myosin and altered gut motility in the klotho model of premature aging. *Neurogastroenterol Motil* 23: e309-323, 2011.
26. Kang JM, Kim N, Kim JH, Oh E, Lee BY, Lee BH, Shin CM, Park JH, Lee MK, Nam RH, Lee HE, Lee HS, Kim JS, Jung HC, and Song IS. Effect of aging on gastric mucosal defense mechanisms: ROS, apoptosis, angiogenesis, and sensory neurons. *Am J Physiol Gastrointest Liver Physiol* 299: G1147-1153, 2010.
27. Wang XY, Huizinga JD, Diamond J, and Liu LWC. Loss of intramuscular and submuscular interstitial cells of Cajal and associated enteric nerves is related to decreased gastric emptying in streptozotocin-induced diabetes. *Neurogastroenterol Motil* 21: 2009.
28. Mansuroglu T, Ramadori P, Dudas J, Malik I, Hammerich K, Fuzesi L, and Ramadori G. Expression of stem cell factor and its receptor c-Kit during the development of intrahepatic cholangiocarcinoma. *Lab Invest* 89: 562-574, 2009.
29. D'Allard D, Gay J, Descarpentries C, Frisan E, Adam K, Verdier F, Floquet C, Dubreuil P, Lacombe C, Fontenay M, Mayeux P, and Kosmider O. Tyrosine kinase inhibitors induce down-regulation of c-Kit by targeting the ATP pocket. *PloS one* 8: e60961, 2013.
30. Santer RM, and Baker DM. Enteric neuron numbers and sizes in Auerbach's plexus in the small and large intestine of adult and aged rats. *J Auton Nerv Syst* 25: 59-67, 1988.
31. Izbeki F, Asuzu DT, Lorincz A, Bardsley MR, Popko LN, Choi KM, Young DL, Hayashi Y, Linden DR, Kuro-o M, Farrugia G,

and Ordog T. Loss of Kitlow progenitors, reduced stem cell factor and high oxidative stress underlie gastric dysfunction in progeric mice. *J Physiol* 588: 3101-3117, 2010.

32. Sekiya M, Hiraishi A, Touyama M, and Sakamoto K. Oxidative stress induced lipid accumulation via SREBP1c activation in HepG2 cells. *Biochem Biophys Res Commun* 375: 602-607, 2008.
33. Miyake H, Inaba N, Kato S, and Takeuchi K. Increased susceptibility of rat gastric mucosa to ulcerogenic stimulation with aging. Role of capsaicin-sensitive sensory neurons. *Dig Dis Sci* 41: 339-345, 1996.
34. Kim SJ, Park JH, Song DK, Park KS, Lee JE, Kim ES, Cho KB, Jang BK, Chung WJ, Hwang JS, Kwon JG, and Kim TW. Alterations of colonic contractility in long-term diabetic rat model. *J Neurogastroenterol Motil* 17: in press, 2011.
35. Lee HT, Hennig GW, Park KJ, Bayguinov PO, Ward SM, Sanders KM, and Smith TK. Heterogeneities in ICC Ca2+ activity within canine large intestine. *Gastroenterology* 136: 2226-2236, 2009.
36. Sanders KM, Koh SD, and Ward SM. Interstitial cells of cajal as pacemakers in the gastrointestinal tract. *Annu Rev Physiol* 68: 307-343, 2006.
37. Hirota S, Isozaki K, Nishida T, and Kitamura Y. Effects of loss-of-function and gain-of-function mutations of c-kit on the gastrointestinal tract. *J Gastroenterol* 35 Suppl 12: 75-79, 2000.
38. Lin L, Xu LM, Zhang W, Ge YB, Tang YR, Zhang HJ, Li XL, and Chen JD. Roles of stem cell factor on the depletion of interstitial cells of Cajal in the colon of diabetic mice. *Am J Physiol Gastrointest Liver Physiol* 298: G241-247, 2010.
39. Rich A, Miller SM, Gibbons SJ, Malysz J, Szurszewski JH, and Farrugia G. Local presentation of Steel factor increases

expression of c-kit immunoreactive interstitial cells of Cajal in culture. *Am J Physiol Gastrointest Liver Physiol* 284: G313-320, 2003.

40. **Wu JJ, Rothman TP, and Gershon MD**. Development of the interstitial cell of Cajal: origin, kit dependence and neuronal and nonneuronal sources of kit ligand. *J Neurosci Res* 59: 384-401, 2000.
41. **Dickens EJ, Edwards FR, and Hirst GD**. Selective knockout of intramuscular interstitial cells reveals their role in the generation of slow waves in mouse stomach. *J Physiol* 531: 827-833, 2001.
42. **Fox EA, Phillips RJ, Byerly MS, Baronowsky EA, Chi MM, and Powley TL**. Selective loss of vagal intramuscular mechanoreceptors in mice mutant for steel factor, the c-Kit receptor ligand. *Anat Embryol (Berl)* 205: 325-342, 2002.
43. **Horvath VJ, Vittal H, Lorincz A, Chen H, Almeida-Porada G, Redelman D, and Ordog T**. Reduced stem cell factor links smooth myopathy and loss of interstitial cells of cajal in murine diabetic gastroparesis. *Gastroenterology* 130: 759-770, 2006.
44. **Gibbons SJ, De Giorgio R, Faussone Pellegrini MS, Garrity-Park MM, Miller SM, Schmalz PF, Young-Fadok TM, Larson DW, Dozois EJ, Camilleri M, Stanghellini V, Szurszewski JH, and Farrugia G**. Apoptotic cell death of human interstitial cells of Cajal. *Neurogastroenterol Motil* 21: 85-93, 2009.
45. **Wouters MM, Gibbons SJ, Roeder JL, Distad M, Ou Y, Strege PR, Szurszewski JH, and Farrugia G**. Exogenous serotonin regulates proliferation of interstitial cells of Cajal in mouse jejunum through 5-HT2B receptors. *Gastroenterology* 133: 897-906, 2007.
46. **Choi KM, Gibbons SJ, Roeder JL, Lurken MS, Zhu J, Wouters MM, Miller SM, Szurszewski JH, and Farrugia G**. Regulation

of interstitial cells of Cajal in the mouse gastric body by neuronal nitric oxide. *Neurogastroenterol Motil* 19: 585–595, 2007.

47. **Young HM, Torihashi S, Ciampoli D, and Sanders KM.** Identification of neurons that express stem cell factor in the mouse small intestine. *Gastroenterology* 115: 898–908, 1998.
48. **Suzuki S, Suzuki H, Horiguchi K, Tsugawa H, Matsuzaki J, Takagi T, Shimojima N, and Hibi T.** Delayed gastric emptying and disruption of the interstitial cells of Cajal network after gastric ischaemia and reperfusion. *Neurogastroenterol Motil* 22: 585–593, e126, 2010.
49. **Choi KM, Gibbons SJ, Nguyen TV, Stoltz GJ, Lurken MS, Ordog T, Szurszewski JH, and Farrugia G.** Heme oxygenase–1 protects interstitial cells of Cajal from oxidative stress and reverses diabetic gastroparesis. *Gastroenterology* 135: 2055–2064, 2064 e2051–2052, 2008.
50. **Lefebvre RA, Dick JM, Guerin S, and Malbert CH.** Influence of the selective neuronal NO synthase inhibitor ARL 17477 on nitrergic neurotransmission in porcine stomach. *Eur J Pharmacol* 525: 143–149, 2005.
51. **McCloskey KD, Anderson UA, Davidson RA, Bayguinov YR, Sanders KM, and Ward SM.** Comparison of mechanical and electrical activity and interstitial cells of Cajal in urinary bladders from wild–type and W/Wv mice. *Br J Pharmacol* 156: 273–283, 2009.

국문 초록

노화에 따른 쥐 대장 근층의 지방 축적과 카할 간질세포 및 nNOS 양성 신경세포의 감소

서론: 대장에서 카할 간질세포의 노화에 따른 변화는 거의 알려진 바 없다. 본 연구의 목적은 노령 쥐 대장 근층의 형태학적 변화를 비롯하여 카할 간질세포 및 신경인성 일산화질소 합성효소(nNOS) 양성 신경세포의 노화에 따른 변화를 알아보는 것이다.

방법: 6 주령, 31 주령, 74 주령, 2 년령 F344 쥐의 근위부 대장을 실험에 이용하였다. C-Kit, nNOS 및 synaptophysin 면역화학염색을 통해 노화에 따른 카할 간질세포 및 대장 근층 내 신경의 수와 분포의 변화를 확인하였다. 또한 real-time PCR 을 이용하여 *C-kit, SCF*(stem cell factor)및 *nNOS* 의 mRNA 를 Western blot 실험을 통하여 c-Kit, nNOS 단백질을 각각 정량 하였다. 노화에 따른 기능적 변화를 알아보기 위해, 각 주령별로 등용성 근수축력을 측정하고 전기자극에 따른 근수축의 변화를 확인하였다.

결과: 근위부 대장 근육 내 지방 축적이 31 주령 이후, 노화에 따라 유의하게 증가하였다. 면역 염색 결과 c-Kit 양성 카할 간질세포 및 nNOS 양성 신경세포 및 신경섬유 역시 주령이 증가할수록 감소하는 양상을 보였다. c-kit 및 nNOS 의 mRNA 와 단백질도 주령이 증가하면서 감소하였다. 자발적 근수축력은 노령 쥐에서 감소하였으며, atropine 및 L-NG-Nitroarginine methyl ester 투여 후 전기자극에 대한 반응은 노령 쥐에서 모두 증가하는 양상을 보였다.

결론: 노령 쥐 대장 근층 내 지방 축적이 증가하고, 카할 간질 세포 및 nNOS 양성 신경세포및 신경섬유의 밀도가 감소하는 현상을 통해 노화로 인한 대장 운동 이상을 일부 설명할 수 있다.

주요어 : 노화, 대장, 카할 간질세포, 신경인성 일산화질소 합성효소, F344 쥐

학 번 : 2011-30579

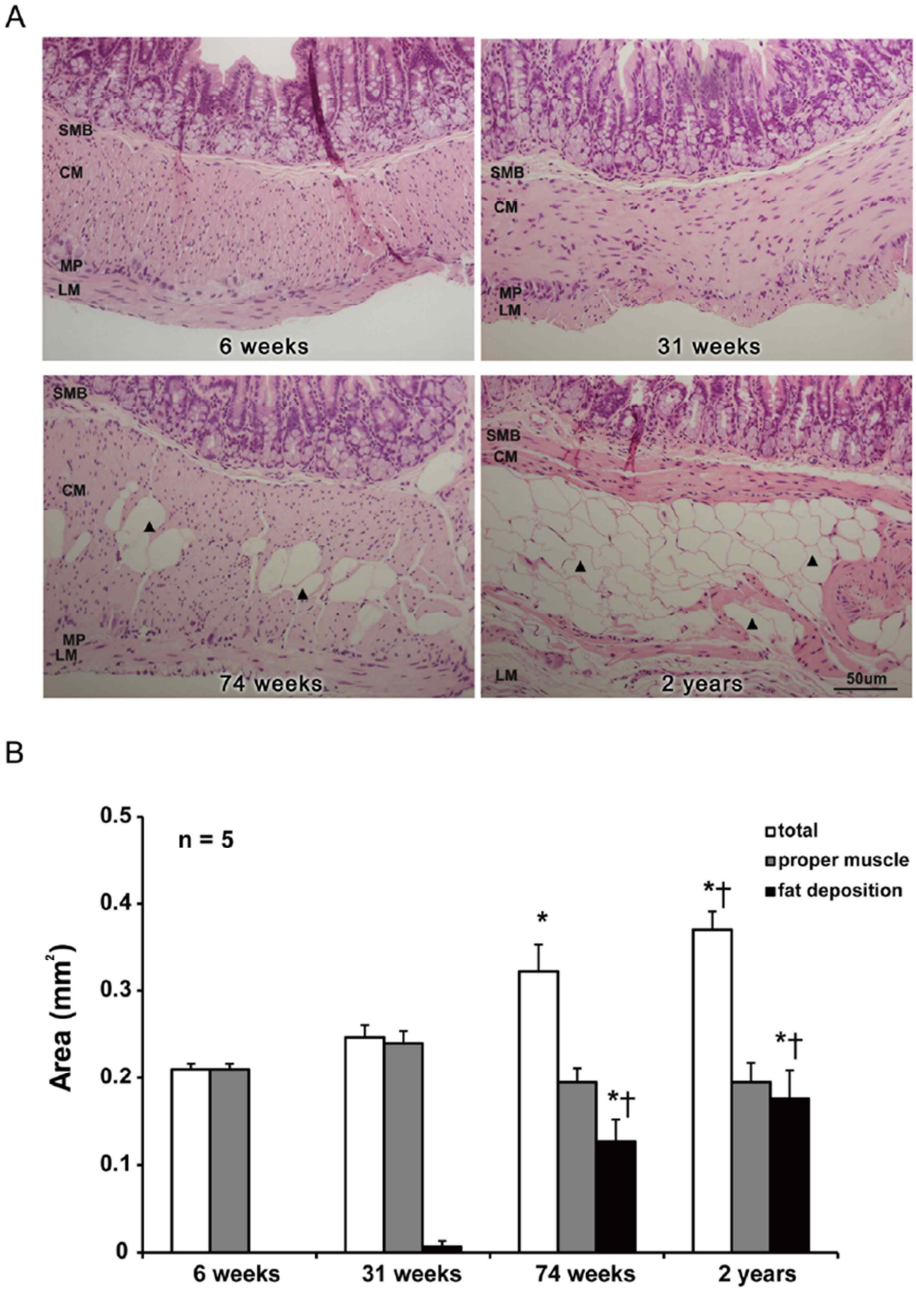

Fig. 1. The change of histology of tunica muscularis according to aging. *(A)* H&E stain (x 200 magnifications) and *(B)* statistical analysis for the measurement of each area. Total smooth muscle area and fat deposition (arrowhead) increased with age (P <0.001) but there was no

significant change in proper smooth muscle area ($P = 0.296$). Results are mean ± SE from 4to 6 animals per group. SMB, submucosal border; CM, circular muscle; MP, myenteric plexus; LM, longitudinal muscle. $^{*}P < 0.05$ compared with 6 weeks of age; $^{\dagger}P < 0.05$ compared with 31 weeks of age.

A

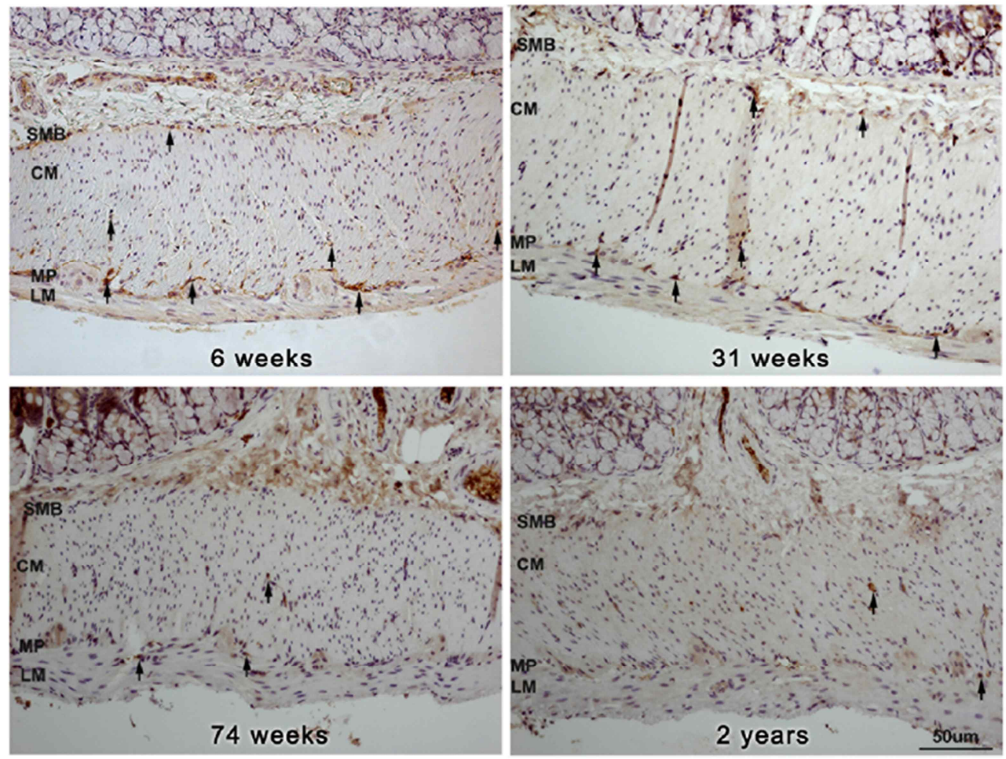
SMB
CM
MP
LM
6 weeks
SMB
CM
MP
LM
31 weeks
SMB
CM
MP
LM
74 weeks
SMB
CM
MP
LM
2 years
50um

B

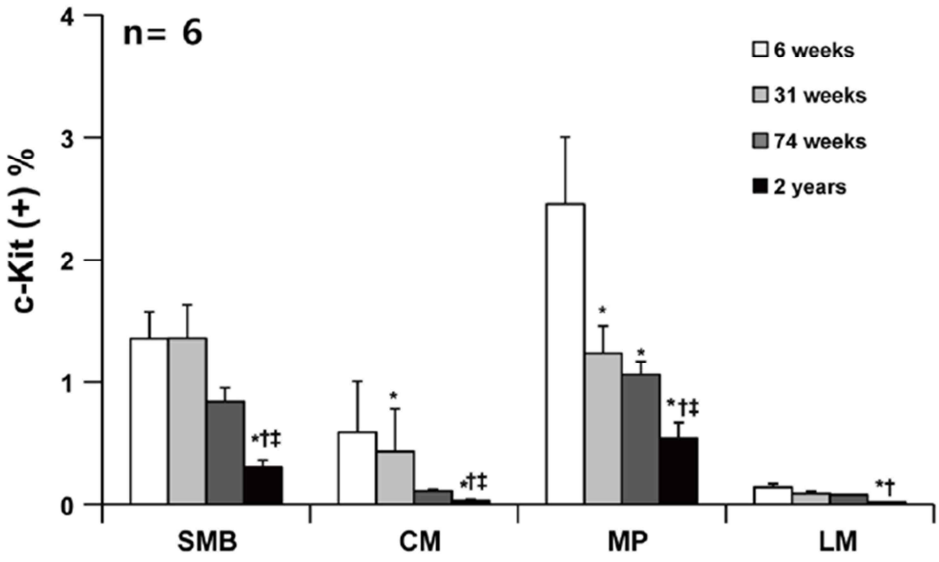
n= 6
c-Kit (+) %
4
3
2
1
0
6 weeks
31 weeks
74 weeks
2 years
*†‡
*
*†‡
*
*
*†‡
*†
SMB
CM
MP
LM

Fig. 2. Analysis of c-Kit immunohistochemistry. *(A)* Photomicrography of c-Kit immunostain of the proximal rat colon. Arrows indicate the c-Kit immunoreactive cell (x200 magnification). (*B*) The comparison of the proportion of c-Kit immunoreactivearea of SMB, MP, CM and LM in 6-, 31-, 74-weeks and 2-years-old rats (each group, $n = 6$). The proportion of c-Kit immunoreactive area showed the tendency to decrease with aging. The result was expressed as c-Kit positive percentage of total area of each region. Each bar represents the mean ± SE. SMB, submucosal border; MP, myenteric plexus; CM, circular muscle; LM, longitudinal muscle. $^{*}P < 0.05$ compared with 6-weeks of age; $^{\dagger}P < 0.05$ compared with 31 weeks of age; $^{\ddagger}P < 0.05$ compared with 74 weeks of age.

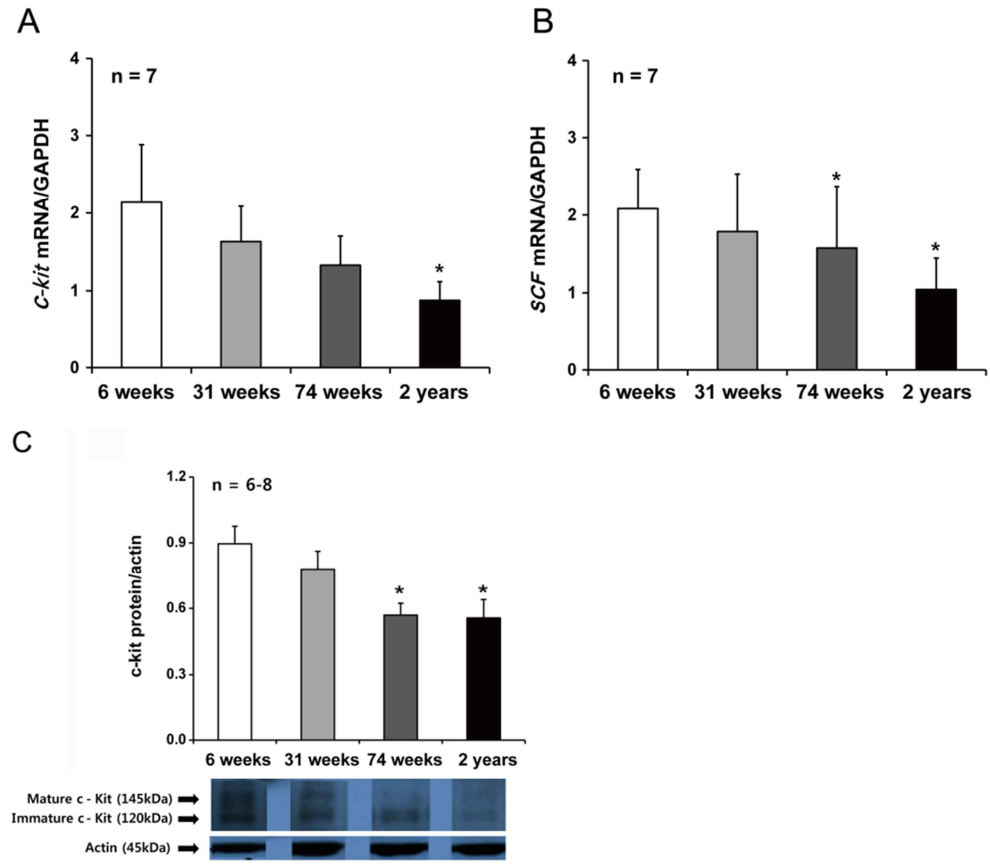

Fig. 3. The expression of *c-kit* mRNA, *SCF* mRNA and c-Kit protein. *(A)* The expression of *c-kit* mRNA by real-time PCR decreased with aging. That of 2-years-old rats significantly decreased compared to the 6-weeks-old rats ($P = 0.035$) (each group, n = 7). *(B) SCF* mRNA expression of 74-weeks and 2-years-old rats was significantly lower than that of 6-weeks-old rats ($P = 0.048$, $P = 0.002$, respectively) (each group, n = 7). *(C)* c-Kit protein expression decreased with aging. c-Kit protein expression of 74-weeks and 2-years old rats was lower than that of 6-weeks-old rats ($P = 0.015$ and $P = 0.029$, respectively) (n = 6 in 6-, 31- and 74 weeks, n=8 in 2 years). Results are shown as a mean value of the optical density (OD). Each of the optical density of mature (145 kDa) and immature (120 kDa) forms was combined into one in the analysis process using densirometry. Each bar represents the mean ± SE. $^{*}P < 0.05$ compared with 6-weeks of age.

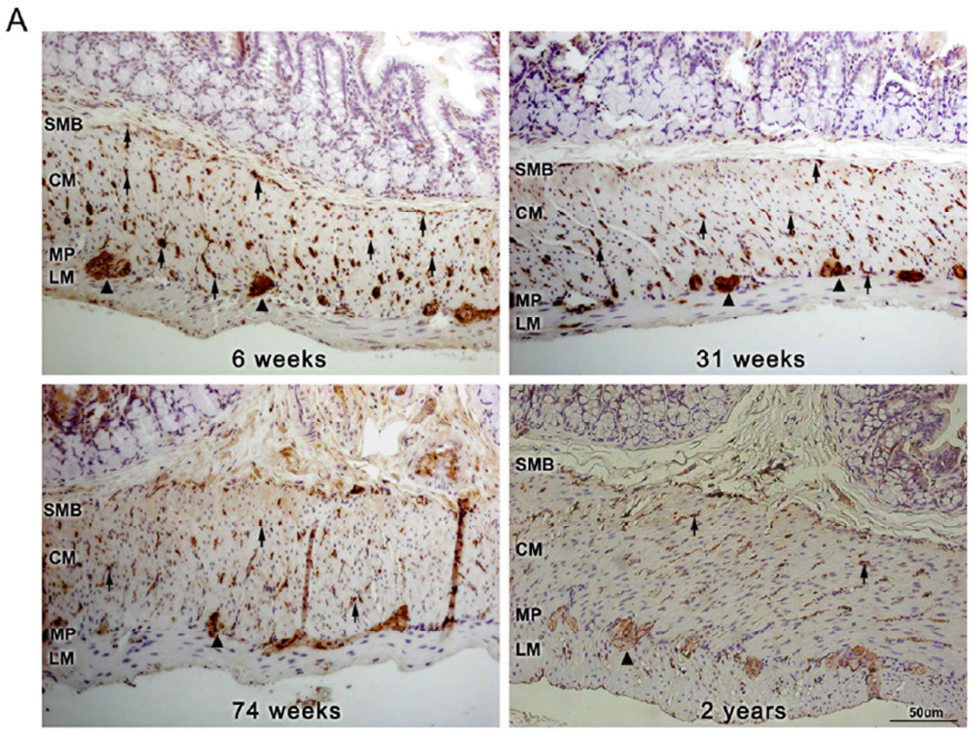
A
SMB
CM
MP
LM
6 weeks
SMB
CM
MP
LM
31 weeks
SMB
CM
MP
LM
74 weeks
SMB
CM
MP
LM
2 years
50um

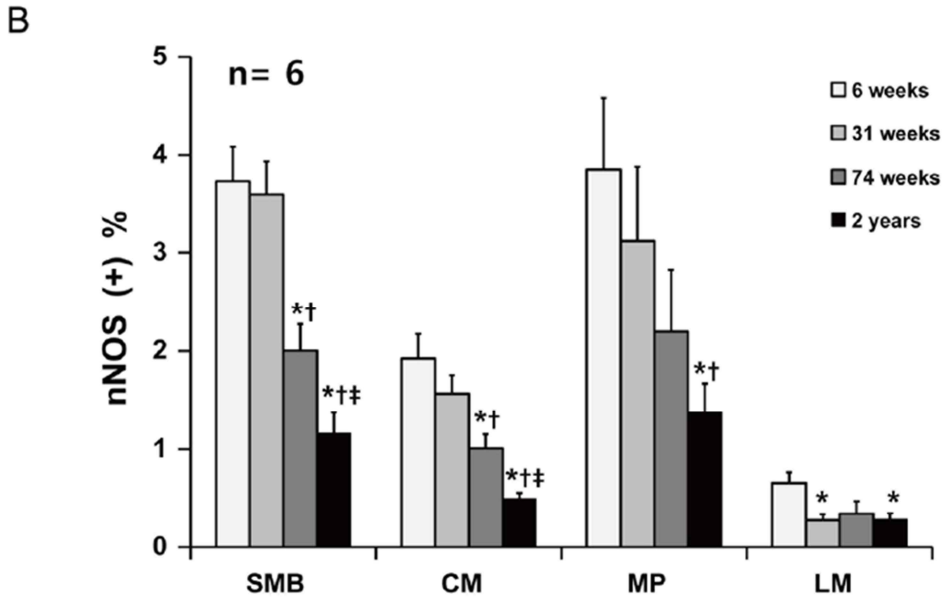
B
n= 6
6 weeks
31 weeks
74 weeks
2 years
nNOS (+) %
0
1
2
3
4
5
*†
*†‡
*†
*†‡
*†
*
*
SMB
CM
MP
LM

Fig. 4. Analysis of nNOS immunohistochemistry. *(A)* Photomicrography of nNOS immunostain of the proximal rat colon. Arrows and arrowheads indicate the nNOS positive nerve fibers and neuronal ganglion, respectively (x200 magnification). *(B)* The comparison of the nNOS positive area (each group, n = 6). The proportion of nNOS immunoreactive area showed the decreasing pattern with aging. Each bar represents the mean ± SE. SMB, submucosal border; MP, myenteric plexus; CM, circular muscle; LM, longitudinal muscle. $^{*}P < 0.05$ compared with 6-weeks of age; $^{\dagger}P < 0.05$ compared with 31 weeks of age; $^{\ddagger}P < 0.05$ compared with 74 weeks of age.

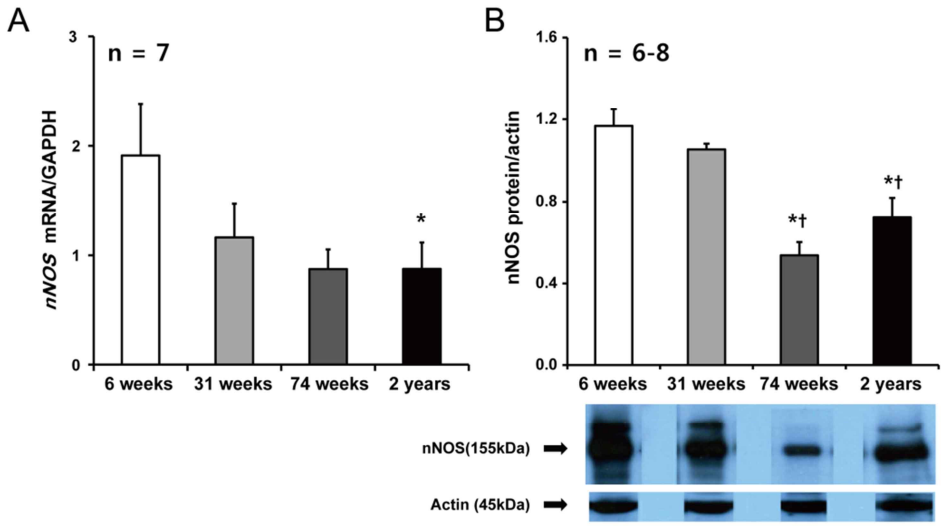

Fig. 5. The expression of *nNOS* mRNA and nNOS protein. *(A)* The expression of *nNOS* mRNA by real-time PCR decreased with aging. The expression of *nNOS* mRNA in 2-years-old rats was significantly lower than that of the 6-weeks-old rats ($P = 0.015$) (each group, n = 7). *(B)* nNOS protein expression on 74-weeks and 2-years-old rats showed significantly lower expression than that of the 6 and 31-wewks-old rats ($P < 0.001$ and $P = 0.003$ vs. 6 weeks, $P < 0.001$ and $P = 0.013$ vs. 31 weeks) (n = 6 in 6-, 31- and 74 weeks, n=8 in 2 years). Results are shown as a mean value of the optical density (OD). Each bar represents the mean ± SE. $^{*}P< 0.05$ compared with 6 weeks of age; $^{\dagger}P< 0.05$ compared with 31 weeks of age.

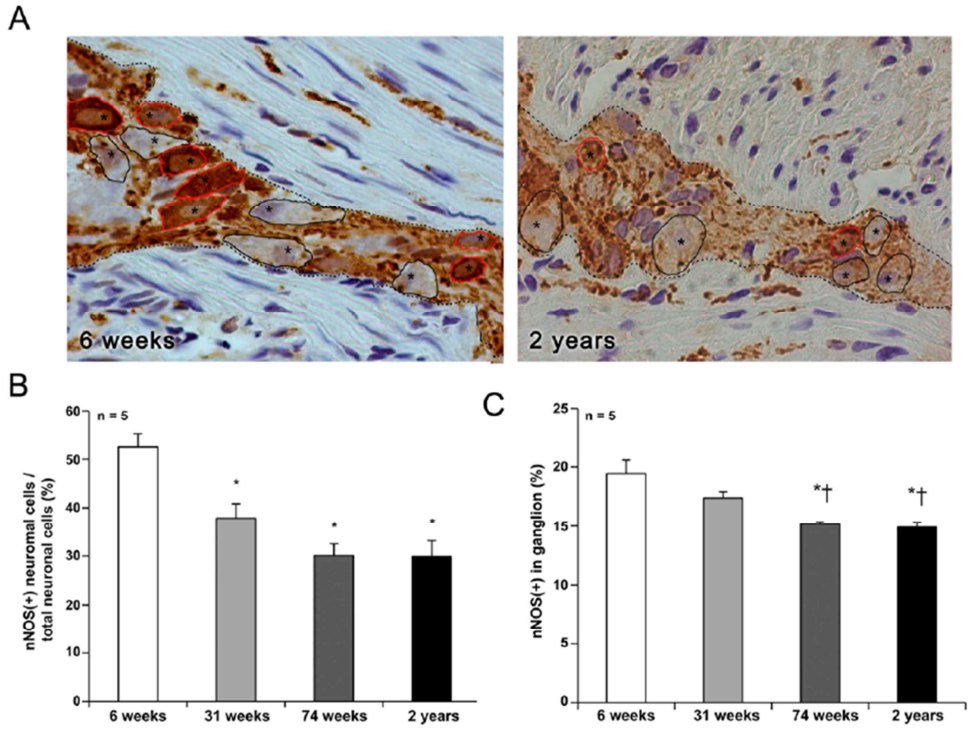

Fig. 6. The enumeration of neuronal cell in myenteric ganglia. *(A)* Ganglia in the myenteric plexus were micrographed at x1,000 (representative pictures of ganglion in 6-weeks and 2-years-old rat are shown). We enumerated the nNOS positive (indicated with red line) or negative (indicated with black line) myenteric neurons, which include nucleus (indicated with star), in the ganglion (contours of the ganglion are indicated by dotted lines). *(B)* The percent of nNOS positive neuronal cells of total neuronal cells in ganglionwas decreased with aging (P = 0.003). *(C)*The mean of proportion of nNOS immunoreactive area in ganglion was also decreased as age increased (P = 0.002). Each bar represents the mean ± SE. $^{*}P < 0.05$ compared with 6-weeks of age; $^{\dagger}P < 0.05$ compared with 31 weeks of age.

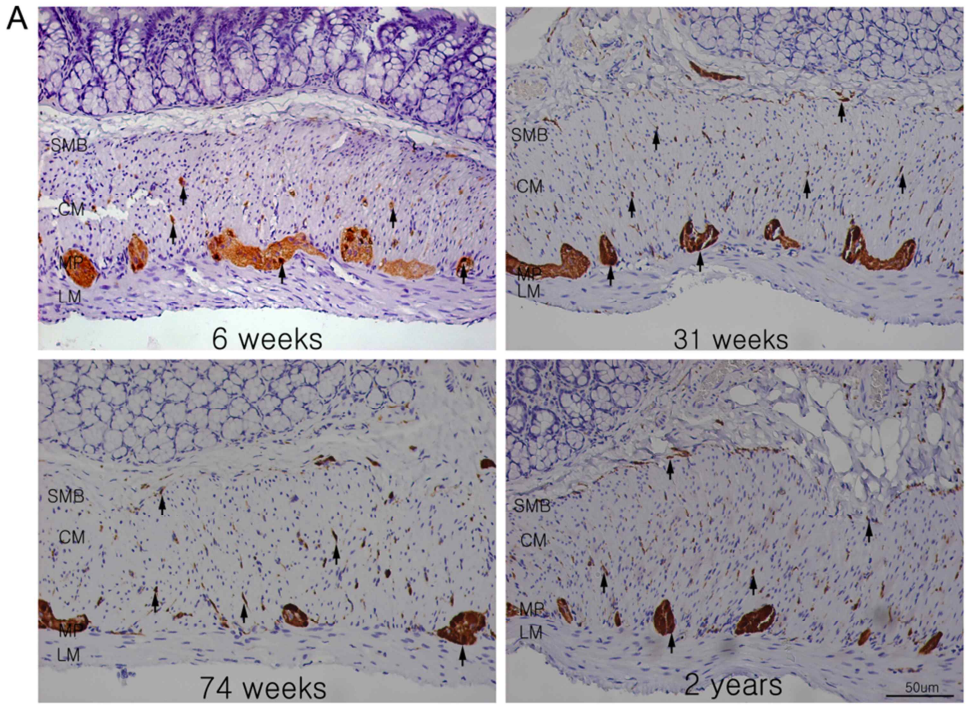
A
SMB
CM
MP
LM
6 weeks
31 weeks
74 weeks
2 years
50um

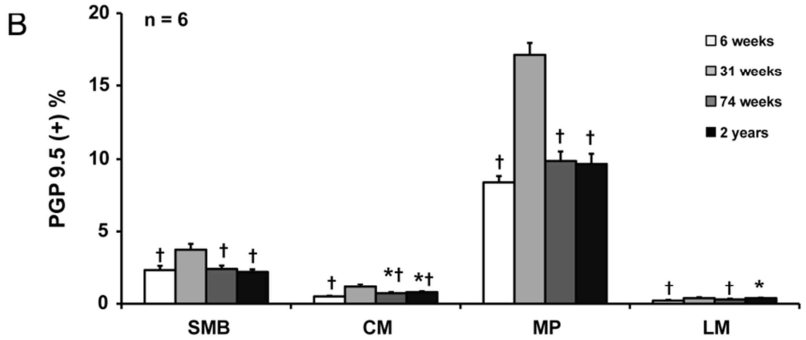
B
n = 6
PGP 9.5 (+) %
20
15
10
5
0
6 weeks
31 weeks
74 weeks
2 years
SMB
CM
MP
LM

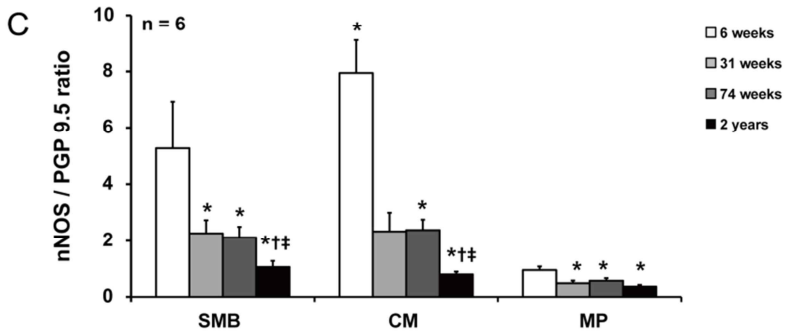
C
n = 6
nNOS / PGP 9.5 ratio
10
8
6
4
2
0
6 weeks
31 weeks
74 weeks
2 years
SMB
CM
MP

Fig. 7. Analysis of PGP 9.5 immunohistochemistry. *(A)* Photomicrography of PGP 9.5 immunostain of the proximal rat colon. Arrows indicate the PGP 9.5 immunoreactive nerve fibers and neuronal ganglion (x200 magnification). *(B)* The comparison of the PGP 9.5 positive area (each group, $n = 6$). The proportion of PGP 9.5 immunoreactive area showed the peak level in the 31-weeks-old rats and that of 74-weeks and 2-years-old rats decreased to the level of 6-weeks-old rats. *(C)* The comparison of ratio nNOS-positive area to PGP 9.5-positive area (each group, $n = 6$). 6-weeks-old rats showed the peak level with statistical significance and the relative ratio of nNOS/PGP 9.5 of 2-years-old rats was lower than that of other age groups (In SMB and CM, both $P < 0.001$ vs. 6 weeks, $P = 0.017$ and $P = 0.001$ vs. 31 weeks, $P = 0.004$ and $P < 0.001$ vs. 74 weeks; in MP, $P < 0.001$ vs. 6 weeks). The result was expressed as percentage of immunostain-positive area to total area of each region. Each bar represents the mean ± SE. SMB, submucosal border; MP, myenteric plexus; CM, circular muscle; LM, longitudinal muscle. $^{*}P < 0.05$ compared with 6-weeks of age; $^{\dagger}P < 0.05$ compared with 31 weeks of age; $^{\ddagger}P < 0.05$ compared with 74 weeks of age.

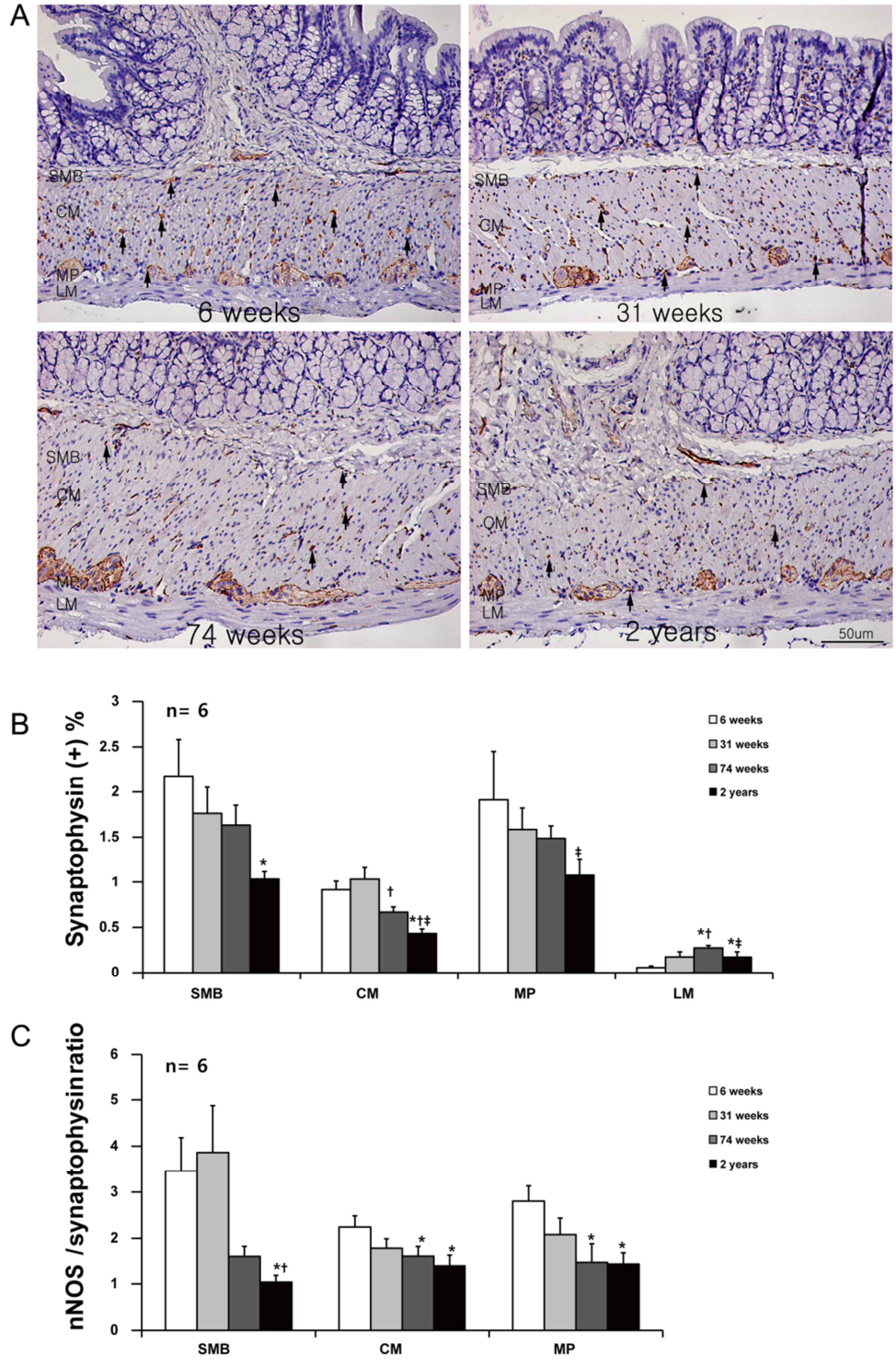
A
SMB
CM
MP
LM
6 weeks
31 weeks
74 weeks
2 years
50um
B
n= 6
Synaptophysin (+) %
6 weeks
31 weeks
74 weeks
2 years
SMB
CM
MP
LM
C
n= 6
nNOS /synaptophysinratio
SMB
CM
MP

Fig. 8. Analysis of synaptophysin immunohistochemistry. *(A)* Photomicrography of synaptophysin immunostain of the proximal rat colon. Arrows indicate the synaptophysin immunoreactive nerve fibers and neuronal ganglion (x200 magnification). (*B*) The comparison of the synaptophysin-positive area (each group, $n = 6$). (*C*) The comparison of ratio nNOS to synaptophysin-positive area (each group, $n = 6$). The result was expressed as percentage of immunostain-positive area to total area of each region. Each bar represents the mean ± SE. SMB, submucosal border; MP, myenteric plexus; CM, circular muscle; LM, longitudinal muscle. $^{*}P < 0.05$ compared with 6-weeks of age; $^{\dagger}P < 0.05$ compared with 31 weeks of age; $^{\ddagger}P < 0.05$ compared with 74 weeks of age.

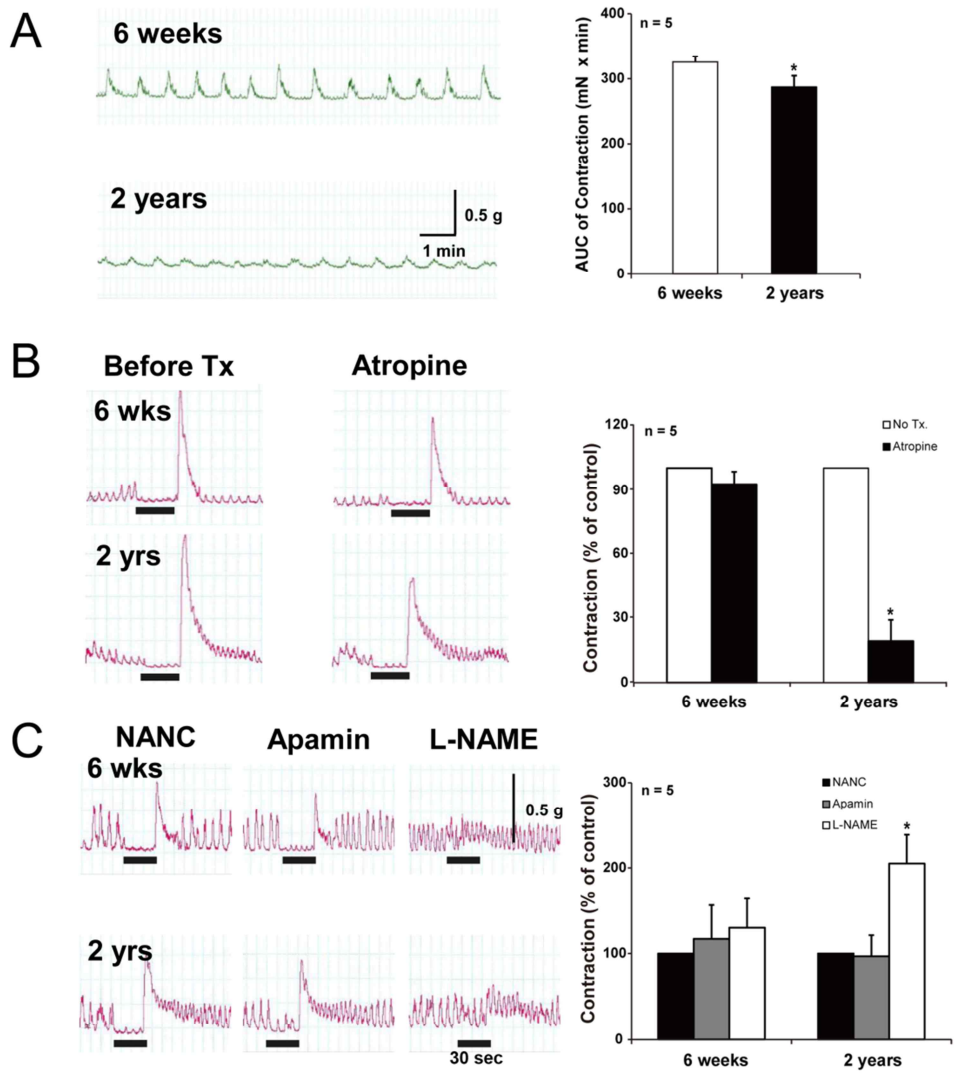

Fig. 9. Isovolumetric contractile measurement and electrical field stimulation. *(A)* The AUC of the spontaneous contractile response in resting state. The responses were significantly decreased in 2-years-old-rat colon (6-weeks-old rats 325.8 ± 8.9 vs. 2-years-old rats 287.2 ± 17.3 mN x min) ($P = 0.032$). $^{*}P < 0.05$ compared with 6 weeks of age. *(B)* The AUC of EFS during the contractile recordings. Colonic muscle contraction in 2-years-old rats was significantly inhibited by atropine

(10μM) (P = 0.000). $^{*}P < 0.05$ compared with no treatment. *(C)* The EFS responses of apamin and L-NAME under NANC condition. L-NAME (1μM) pretreatment significantly increased contractility in 2-years-old rats compared with the 6-weeks-old rats (P = 0.000). $^{*}P < 0.05$ compared with NANC condition. EFS, electrical field stimulation; NANC condition, non-adrenergic, non-cholinergic condition.